FUEL CELL
RESEARCH & DEVELOPMENT

RESEARCH ON COMPACT FUEL CELL POWER SUPPLIES

PROGRESS REPORT NUMBER 1

FOR

WORK PERIOD ENDING - SEPTEMBER 30, 1960

CONTRACT NO. DA-19-129-QM-1705

U.S. ARMY

QUARTERMASTER RESEARCH AND ENGINEERING COMMAND

NATICK, MASSACHUSETTS

D D C
RECEIVED
AUG 7 1969
B

AIRCRAFT ACCESSORY TURBINE DEPARTMENT

GENERAL ELECTRIC

52

RESEARCH ON COMPACT
FUEL CELL POWER SUPPLIES

By

AIRCRAFT ACCESSORY TURBINE DEPARTMENT
FUEL CELL LABORATORY

PROGRESS REPORT NO. 1

WORK PERIOD ENDING - SEPTEMBER 30, 1960

For

U. S. ARMY
QUARTERMASTER RESEARCH AND ENGINEERING COMMAND
NATICK, MASSACHUSETTS

AIRCRAFT ACCESSORY TURBINE DEPARTMENT
GENERAL ELECTRIC COMPANY
LYNN, MASSACHUSETTS

TABLE OF CONTENTS

TABLE OF CONTENTS (Cont'd)

INTRODUCTION

This is a technical progress report of a research program directed toward improvement of the Ion-Exchange Membrane Fuel Cell concept. This work is conducted by the General Electric Company under contract No. DA-19-129-QM-1705 with the U. S. Army Quartermaster Research and Engineering Command. The objective of this program is to:

> "Initiate research studies to establish those factors which currently contribute the high energy losses of the ion-exchange membrane and establish approaches to minimizing such losses to achieve substantially greater power densities per unit weight of cell."

In this series of reports, progress is reported on work directed toward the above objective. In addition, progress is reported on certain related work being conducted at the Aircraft Accessory Turbine Department. This is made possible by virtue of the similarity of the objective of this contract with that of other work being conducted concurrently. The Work Plan for the total work reported is given in section 0.4 of this report. Guidance and approval of the direction of the work under this contract is given by Mr. L. A. Spano - Chief, Advanced Projects Office, Quartermaster Research and Engineering Command, Natick, Massachusetts.

These progress reports are issued on a bi-monthly basis and special summary reports issued as indicated. The reader should recognize that this is a progress report covering a particular period of time. The experiments reported are factual, but not necessarily complete, and any conclusions made must be considered tentative until a summary report is issued. Comments and suggestions on these reports are most welcome.

0.2 SUMMARY

During the first two months of the contracted work, significant progress has been made in the quantitative description of the various ohmic losses present in the G. E. ion-exchange fuel cell. Slow electrochemical polarization has been separated from the ohmic losses present in a cell by using a Kordesch-Marko Bridge, and the value of these losses were confirmed by a separate A. C. bridge measurement. Methods for measuring the characteristic resistance of most of the cell's components have been reported. Finally, a method of characterizing the multi-layer reinforced ion-exchange membrane, as made up of a series of characteristic resistances associated with each impregnated ply of reinforcing, is presented. Although data are only approximate, results indicate the usefulness of this concept in predicting reinforced-membrane ohmic resistances.

The work is on schedule.

0.3 STATEMENT OF WORK

A. SCOPE:

The Contractor shall, commencing on 3 October 1960 and continuing through 2 October 1961, furnish necessary services, labor, materials, tools, equipment and supplies, and will furnish his best efforts to do what is deemed necessary to:

Initiate research studies to establish those factors which currently contribute the high energy losses of the ion-exchange membrane and establish approaches to minimizing such losses to achieve substantially greater power densities per unit weight of cell. The principal effort under this contract should include but not be limited to a study of the factors that impede the conduction of electronic and ionic charges. Investigation of resins, membrane and catalyst formulations and their incorporation into a cell should be conducted to achieve maximum performance.

B. REPORTS:

Reports shall be submitted in accordance with the following:

1. The Contractor shall submit ten (10) copies of Bi-monthly reports within fifteen (15) days following the end of each reporting period, indicating progress of work to date and significant developments. These quarterly reports shall include:
    - a. An estimate of the percentage of work completed to date.
    - b. An estimate of the percentage of costs incurred to date.
    - c. A statement that to the contractor's best knowledge the funds remaining unexpended are sufficient to complete the work called for by the contract, or a revised estimate setting forth the costs required to complete the contract and the reason(s) for the contemplated excess.

2. Upon completion or termination of the contract, the contractor shall furnish fifty (50) copies of a complete final report or summary report which shall consolidate all findings, notes, data, computations, tests procedures, evaluation of all data, test results, principles and techniques relative to the objective indicated herein. The contractor shall include specific conclusions and recommendations concerning work done and detailed information and recommendations relative to further work that may be required. All reports shall be identified with Project No. 7X80-01-New. The final report shall be submitted within thirty (30) days after the expiration or termination date of the contract. Reports shall be of a paper bound brochure type using commercially available bond paper. All reports shall be submitted to the responsible Project Officer, Chemicals & Plastics Division, HQ QMR&E Center, Natick, Massachusetts.

PRIORITY RATING: DD C9E CERTIFIED UNDER DMS REGULATION #1 IS ASSIGNED TO THIS CONTRACT.

PLACE OF PERFORMANCE: Contractor's plant, West Lynn, Massachusetts.

0.4 WORK PLAN

REGULATED, COMPACT FUEL CELL POWER SUPPLIES

General Objective

Conduct a research and development program to achieve the capability of designing compact, lightweight and reliable, regulated fuel cell power supplies.

Research Approach

Task I
Studies of Contributions to and efforts to minimize electronic and ion impedances.

A. Quantitative studies of contributions to electrical losses in present cells.

1. Separate ohmic losses from electrochemical irreversibilities by use of an adaptation of the Kordesch-Marko bridge and other electronic techniques.

2. Determine magnitude of various contributions to ohmic impedance by independent measurements of electrode-layer resistance, current-collector resistance, contact resistance, and electrolytic conductivity of the membranes. Establish apparent ohmic resistance attributable to electrolytic conductivity of the membranes by other methods, including multi-frequency A. C. bridge measurements and driven-cell D. C. resistance with two hydrogen electrodes.

B. Minimization of electrolytic conductance losses.

1. Investigate ion-exchange resin formulations with varying exchange capacities, ionization constants and water content with regard to their effect on cell performance.

2. Investigate the effect on cell performance of membrane thickness along with varying the amount and distribution of resin and reinforcing material.

3. Evaluate various reinforcing materials from the standpoint of cell performance, strength, compatibility, and ease of membrane manufacture.

C. Minimization of electronic losses.

1. Investigation of catalyst impregnated carbon electrodes to minimize electrode layer resistance.

2. Evaluate various carbon blacks with different catalyst loadings and physical properties with regard to cell performance and life.

Task II

Study of the internal generation and storage of hydrogen fuel

A. Studies at the Electronics Laboratory, HMED, Syracuse, of palladium and other absorbents.

B. Provision of data by the AAT Laboratory on the electrolysis characteristics of membrane fuel cells, including details of supplying the water required for such operation.

Task III

Study of the external generation and storage of hydrogen and oxygen

A. Electrolytic methods. Engineering work leading to the development of a prototype model of a small high pressure electrolyzer. The initial design concept is that of a compartmented vessel for simultaneous generation and containment of hydrogen and oxygen in quantities sufficient for operation of a fuel cell for a specified duty cycle. Included will be studies of pressure reduction methods including minimum weight regulators of conventional design.

B. Chemical Methods. Studies of various chemical systems for minimum volume and cost hydrogen generators. The size will be set by the required duty cycle. Noxious reaction products are to be avoided. Feasibility of the process using the best of the chemical system(s) will be demonstrated by constructing a laboratory model generator including pressure regulators as required.

1.0 BACKGROUND

A fuel cell is a device which accomplishes the electro-chemical conversion of the chemical energy of a fuel, directly into useful electrical energy. Depending upon the type of fuel and principle of operation, the device can be rather complex because of physical and chemical limitations. However, the conversion process, utilizing the ion exchange membrane as a solid electrolyte offers very nearly the ultimate in design and operation simplicity for the hydrogen-oxygen cell.

1.1 ION EXCHANGE MEMBRANE FUEL CELL

In the ion exchange membrane fuel cell, a supply of hydrogen and oxygen gases are supplied for either side of an ion exchange membrane at essentially atmospheric pressure. The membrane is faced on either side with a current collector or a similar type of electrode. A catalyst facilitates the chemical reactions at the electrodes. At the anode, the hydrogen is oxidized, forming hydrogen ions that enter the membrane electrolyte and electrons that pass out through the external electric circuit. The hydrogen ions migrate through the ion exchange membrane to the oxygen electrode, the cathode of the cell. At the cathode, oxygen is reduced by the electrons from the external circuit and water is formed by combination with the hydrogen ions from the electrolyte. The water is then easily drawn off or evaporated. The overall result is the controlled chemical combination of hydrogen and oxygen to form water with the release of useful electrical energy.

A more detailed technical description of the ion exchange membrane fuel cell is included in the appendix to this report. The two papers contained in this pamphlet review the development and status of this fuel cell as of May 18, 1960.

1.2 DISCUSSION OF WORK PLAN

Previous work in the area of cell performance improvement has been largely directed toward a specific product application. Of necessity this required a rather cursory approach to investigating cell construction and arrangements. It is expected that with a more systematic program of investigation, such as proposed here, it will bring understanding which will allow optimized fuel cells of significant power density capability. In this program it is proposed that work be started by the study of present cell construction with the anticipation that this will be used as a base from which further improvements in power density will be achieved.

First in such a program, should be the quantitative assessment and analysis of electrical losses in the present manufactured cells. This work should separate the ohmic losses from the various electrochemical losses present using some simple means such as an adaptation of the Kordesch-Marko bridge. By performing certain other AC and DC electrical measurements, these ohmic losses can be further subdivided into resistances attributable to current-collectors, collector contact with the membrane cell, membrane electrode-layer resistances and "solid" electrolyte resistances. With this information in hand, it will be possible to assess the probability of reducing certain of these electrical losses.

Development work recently accomplished has led us to believe that one source of these electrical losses in the present cell can be easily reduced. The area is identified with electrolyte conductance losses. Some types of reinforced ion-exchange cell constructions have shown an increase in performance on air of about fifty percent over the present type of standard cell construction. In this program, we propose to investigate these and other cell constructions in order to gain some understanding of the effect and to improve cell performance with respect to these parameters. This investigation is well suited to the present proposed program because the wo rk is in part straight-forward and therefore can be programmed with a fair chance of successfully accomplishing the goals.

Three areas of electrolyte construction will be investigated to determine their effect on cell performance. First, using both heterogeneous and homgeneous membrane construction techniques, we will change the amount of ion-exchange capacity, water content, and functional group ionization constant present in the resinous electrolyte in an effort to gain an insight into the operating mechanisms. Secondly, with one type of resin and reinforcing, we will vary the membrane thickness as well as the distribution of resin and reinforcing material. Also work concerning different types of reinforcing will be undertaken. In our prior work, we have seen evidence that these membrane parameters affect cell performance. Therefore an optimization should be accomplished.

Finally the reader will find the work elements necessary to determine the feasibility of using types of special carbons as an electron-conducting catalyst-supporting electrode, constructed in such a manner as to be permeable to gasses. The electron-conductance requirements of the electrode layer, established early in this program will be a valuable guide in selecting the proper type of carbon. It would be desirable to incorporate carbons into the present fuel cell to allow more efficient utilization of the more expensive catalysts for greater performance. In addition, this lends to providing a good-conducting inert electrode that can act as a catalyst support for a wide variety of distributed catalysts to further increase the probability of improved performance.

Future investigations, not included in this present study, could then concern itself with distributed catalyst development. Perhaps these catalysts, distributed in molecular layer on a selected carbon, would be somewhat freed of as high a requirement of good electrical conductance as the present catalysts which must act as both the electron carrier and reaction promoter.

It is reasonable to assume that optimization studies such as this one will lead to power densities over 25 watts per sq. ft. with membrane cells only 10 mils thick. Such cells, when assembled into compact structures capable of porting in gases and ridding themselves of water as a product, will have power densities near 2 KW per cubic foot. This power density is about five times higher than values for the bulk of cells and structures currently manufactured.

The working arrangements proposed to accomplish this program are as follows: Technical direction and personnel supervision will be given by Dr. E. A. Oster, drawing upon the technical abilities of the group residing in Dr. P. V. Popat, Dr. H. J. R. Maget, and Dr. R. B. Hodgdon to interpret information they and others gather in the program. The principal experimental investigator will be A. P. Fickett who will be responsible for experiments and integrating the information into a consistent set of facts.

Laboratory assistants will be assigned to these men to the extent that is required and the program funding allows.

1.3 ORIENTATION TO THIS WORK

The performance of any fuel cell system may be defined in terms of its current and voltage output. For a theoretically perfect fuel cell, the voltage obtained would be the thermodynamically reversible voltage of the fuel and oxidizer involved, -- approximately 1.23 volts in the case of a hydrogen-oxygen fuel cell operating at one atmosphere pressure near room temperature. In studying ways to increase performance, it is natural that attention be focused on the nature of the deviation of the actual ion exchange fuel cell performance from the ideal fuel cell. In general, inside the cell structure, two effects are responsible for the non-ideal decrease in voltage with increasing current that characterizes all actual fuel cells and batteries. One category of these irreversibilities is the internal cell resistance which is manifested as an ohmic drop across the cell terminals. This ohmic resistance in the ion exchange fuel cell is actually a sum of many smaller resistances such as resin resistance, electro-catalyst resistance, contact resistance, cloth resistance, and fixture resistance which are present in an electrically passive and non-reactive manner. The second effect present inside the cell is the sum of slow irreversible processes which may be electro-chemical in nature and referred to as polarization losses. A plot of voltage versus current, commonly called a total polarization (internal resistance plus electrode polarization) curve, is usually used to represent the performance of the cell. The slope of this curve $\frac{dv}{dI}$ is sometimes called the internal impedance (resistance plus the polarization) of the fuel cell.

Optimization of fuel cell performance requires at some point a complete analysis of the resistance elements. Such an analysis would consist of first separating the ohmic-type irreversibilities from the electrode-polarization type. Next, it is necessary to split the total ohmic resistance to determine the magnitude of the contact resistance, catalyst ohmic resistance, resin resistance, etc., and thus determine those areas which promise the greatest potential for optimization. It is finally necessary to minimize those ohmic resistances which have been determined as the major contributors to the total cell resistance, and in this way obtain part of an optimization of fuel cell performance with respect to a general type of cell construction.

Beside the analysis and optimization of ohmic losses, this study lays the ground-work for a future catalyst-optimization later in the work program which will be started after the selection of a good electro-catalyst carrier or extender. Also later in this study specific investigations are planned into the various methods of generating hydrogen.

2.0 TASK 1A - QUANTITATIVE STUDIES OF ELECTRICAL LOSSES IN PRESENT CELLS

2.1 SEPARATION OF OHMIC LOSSES FROM ELECTRO-CHEMICAL IRREVERSIBILITIES

For the purpose of this contracted work, it was necessary to establish an agreement between several methods of determining the internal ohmic resistance of the General Electric Ion-Exchange Fuel Cell. Agreement between two methods is presented in this report section. A third method depending upon nearly reversible hydrogen electro-catalysis will be evaluated during the next reporting period to complete this area of the original work statement.

2.1.1 THE 60-CYCLE KORDESCH-MARKO BRIDGE

The Kordesch-Marko Bridge is an electrical device which allows the measurement of "slow" cell polarization separated from cell internal ohmic irreversibility. In effect the bridge measures only the slow polarization by allowing the fuel cell to run with continually interrupted direct current. Measurement of cell potential is made at periods when there is no current flowing through the cell. During these times there is no internal resistance manifested in the cell potential but the electrode-polarization processes are too slow to follow the current interruption and are measured as a voltage, deviating from a reference voltage, usually the open circuit voltage. This polarization curve can then be compared to the curve obtained by running the cell on direct current which will measure the sum of the "quick" ohmic losses and the "slow" polarization. Thus the ohmic losses are determined by a voltage difference.

The principle of operation can be seen by referring to Figure I. The transformer "A" would normally deliver a 60 cycle alternating current to the fuel cell through a resistive load but a diode in the series circuit rectifies the current.

The ammeter and potentiometer "A" read the proper <u>average</u> interrupted current and voltage respectively. A curve of such averaged voltage versus averaged current will closely agree with a curve of the same variables obtained by running the cell on direct current which is not interrupted.

Referring to the portion of the circuit including transformer "B" and the fuel cell, one notes that transformer "B" is 180° out of phase with transformer "A", and that potentiometer "B" is connected to the center tap of transformer "B" which is included in a balanced very low-current loop. When transformer "B" operates in a direction to pass through the diodes, the "voltage" signal from the "unrecovered" fuel cell is allowed to pass to the potentiometer "B". A small current will pass through the balance loop only when the current through the cell is zero. During this brief time the cell is essentially put on open circuit because of the high resistance of potentiometer "B" in the balanced loop. As previously noted, the cell cannot recover its open circuit voltage during the short interruption because of the "slow" mechanism of certain types of depolarization. Therefore, the potentiometer "B" can measure the appropriate potential that the cell would have operating with no internal resistance losses.

2.1.2 METHOD OF USING THE KORDESCH-MARKO BRIDGE

In general, the curves obtained by using the interruptor and those obtained from DC measurements will appear as in Figure II. The position of the curves will be a function of time, both curves rising to a steady state value after about one hour of operation per point. However, the distance, $\underline{\Delta}$ **E**, between the curves (at any one value of current density) will remain nearly constant throughout the transient. Thus, the cell resistance can be found rapidly, providing that the potentiometers in the interrupted circuit and the DC circuit are read at the same time. The true electrode polarization curve, however, can be found only by allowing the fuel cell and the measuring circuit to stabilize for one hour at each current density level.

2.1.3 EFFECT OF INTERRUPTOR FREQUENCY

Since the accuracy of measurements using the interruptor technique depends on the inability of the fuel cell mechanisms to recover quickly to open circuit voltage during the current interruption period, an experiment was run to determine if a different result could be obtained by shortening the interruption time. Tests were run using alternating signals of 60, 180, and 240 cycles per second. No difference was noted in the data, indicating that 60 cycle input to the transformer provides sufficient interruption frequency to divide cell irreversibilities into two general categories.

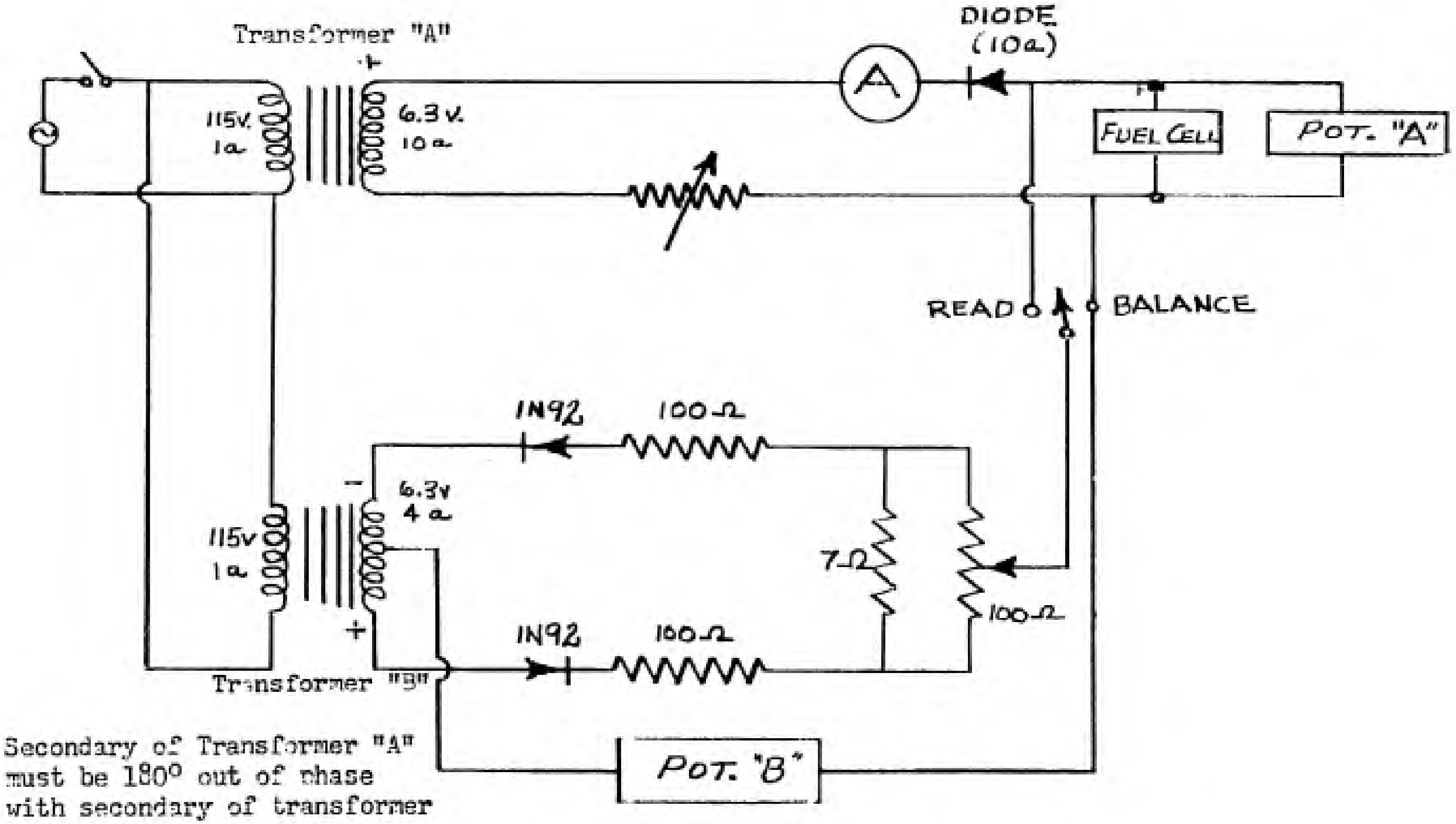

Secondary of Transformer "A" must be 180° out of phase with secondary of transformer "B" as shown.

Figure I

SCHEMATIC OF KORDESCH-MARKO BRIDGE FOR DETERMINING FUEL CELL RESISTANCE

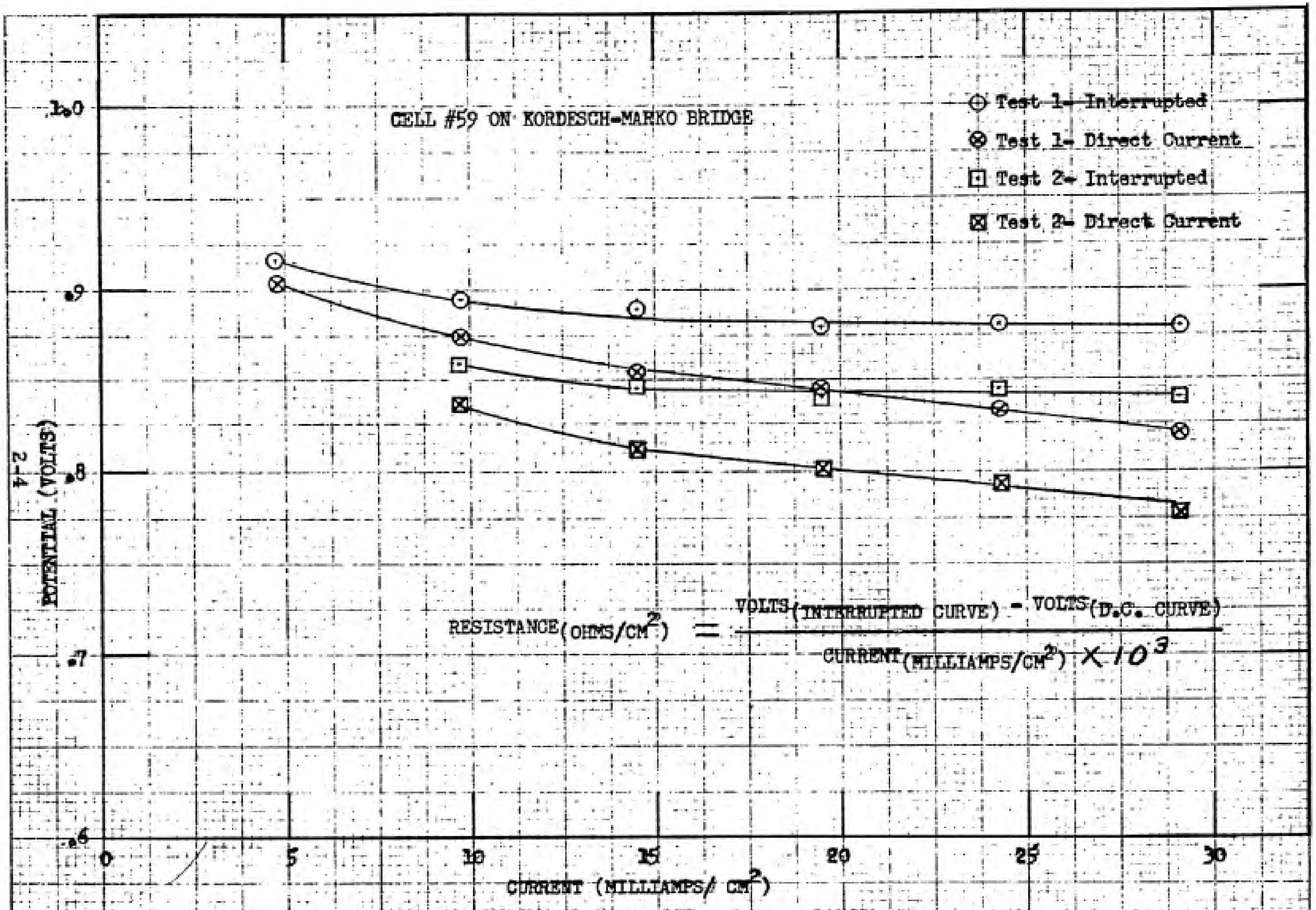
CELL #59 ON KORDESCH-MARKO BRIDGE
⊙ Test 1- Interrupted
⊗ Test 1- Direct Current
⊡ Test 2- Interrupted
⊠ Test 2- Direct Current
RESISTANCE(OHMS/CM²) = VOLTS(INTERRUPTED CURVE) - VOLTS(D.C. CURVE) / CURRENT(MILLIAMPS/CM²) × 10³
POTENTIAL (VOLTS)
1.0
.9
.8
.7
.6
0
5
10
15
20
25
30
CURRENT (MILLIAMPS/ CM²)

Figure II

2.1.4 VARIATIONS IN THE CELL POLARIZATION CURVES

The electrode polarization curve and the d. c. curve as shown on Figure II have been found to vary by about 7 per cent from one test to another if the membrane had been removed from the test fixture between tests and immersed in distilled water. However, the ohmic resistance of the cell does not change even though the cell polarization level changes. All Kordesch-Marko Bridge measurements were made on cells with an active area of 4.35 by 4.35 inches.

2.1.5 REPRODUCIBILITY OF RESISTANCE MEASUREMENTS

The ohmic resistance of two cells was determined several times to evaluate the reproducibility of the results. In Table I, experimental determinations showing the number of measurements, the average resistance, and the percent deviation are presented.

The data at the low current density points (4.86 and 9.72 ma/cm^2) were disregarded since an inherently large error exists when one takes the difference between two potential readings whose values are close to one another. Also there is a slight inherent measurement discrepancy between potential readings at very low current densities with this practical K. M. bridge. At open circuit voltage, a difference of 0.002 volts between potentiometers was noticed; probably inherent in the diode electrical circuit used in the bridge's operation.

The average total resistance calculated from all K. M. bridge readings, excluding the low current density values, was $R_{avg.}$ = 8.08 ohm-cm^2.

The resistance, found independently from several a. c. bridge measurements grouped very closely together, was R - 8.09 ohm-cm^2 (total ohmic losses). No noticeable difference in a. c. resistance is noted if the bridge frequency was 60 or 1,000 cps. Such agreement in total ohmic resistance measurements between the direct a. c. bridge determination and the K. M. bridge difference determination was an objective of Task 1A. A second example of this agreement is reported for Cell 59, a low resistance construction. See Table II. Excluding readings at 4.9 and 9.7 ma/cm^2, the average resistance for all points is $R_{avg.}$ = 2.14 ohm-cm^2.

The resistance obtained by the a. c. resistance bridge was R = 2.13 ohm-cm^2 (total ohmic losses).

TABLE 1 - TOTAL K. M. OHMIC LOSSES FOR CELL 13

Current Density (ma/cm^2)	Number of Points Taken	Average Resistance ohms-cm^2	Average Deviation ohms-cm^2	Average Percent Deviation
TEST NO. ONE				
4.9	--	-	-	-
9.7	3	8.16	± 0.13	± 1.6
14.6	5	8.33	± 0.08	± 1.0
19.4	3	7.96	± 0.24	± 3.0
24.3	3	7.96	± 0.07	± 0.9
29.2	6	7.86	± 0.07	± 0.9
TEST NO. TWO				
4.9	6	7.65	± 0.21	± 2.7
9.7	7	8.20	± 0.19	± 2.3
14.6	7	8.03	± 0.06	± 0.8
19.4	7	8.07	± 0.06	± 0.8
24.3	4	8.12	± 0.03	± 0.4
29.2	12	8.21	± 0.06	± 0.8

TABLE II - TOTAL K.M. OHMIC LOSSES FOR CELL 59

Current Density (ma/cm^2)	Number of Points Taken	Average Resistance ohms-cm^2	Average Deviation ohms-cm^2	Average Percent Deviation
TEST NO. ONE				
4.9	3	2.34	± .02	± 0.9
9.7	6	2.22	± .05	± 2.3
14.6	5	2.16	± .03	± 1.4
19.4	5	2.12	± .01	± 0.5
24.3	7	2.09	± .01	± 0.5
29.2	14	2.11	± .02	± 1.0
TEST NO. TWO				
4.9	2	2.44	± .07	± 3.0
9.7	4	2.37	± .06	± 2.6
14.6	8	2.22	± .03	± 1.4
19.4	17	2.18	± .03	± 1.4
24.3	4	2.09	± .01	± 0.5
29.2	10	2.12	± .03	± 1.5

Thus, these cited data for two cells, having widely different internal resistances, show agreement between the more complex K. M. bridge determination and the more easily obtained laboratory a. c. bridge values. Also by comparing the K. M. bridge values appearing in Tables I and II for reproducibility between the first and second test setup on each cell, one finds values repeating within about one percent when current densities were over 10 ma/cm^2. With the present model a. c. bridge used, a similar reproducibility in resistance measurement between setups of the same cell runs several percent.

2. 2 MAGNITUDE OF OHMIC RESISTANCES

In this first report period, methods have been established to obtain specific-resistance measurements of the individual component parts, present in cell configurations of known total ohmic resistances. These methods have not as yet been completely evaluated. Thus, it would be premature at this time to find any correlation via a mathematical model with the experimental total ohmic resistance of the cells determined by the Kordesch-Marko technique. However, at a later time in this contract when methods and measurements have been improved such a correlation will become the objective of the work.

2. 2. 1 ELECTRO-CATALYST RESISTANCE TO ELECTRON FLOW

The following method, developed by Dr. E. J. Cairns of the Research Laboratory, was used to determine electro-catalyst resistance. A strip, 0. 5 inches wide and 5 or more inches in length, was cut from a catalyst coated membrane, i. e., the cell. The electro-catalyst was completely removed from one side of the membrane strip, and the strip was then placed in the apparatus shown in Photo #3. The gold-plated electrodes were clamped tightly against the catalyst layer on one side of the strip and the resistance measured by an a. c. or d. c. resistance bridge. It should be noted that once the catalyst was removed from the other side of the strip, either a. c. or d. c. resistance measurements were adequate for the following reasons:

1. An a. c. resistance bridge will measure the catalyst and resin resistances in parallel. However, the resin resistance is 100 times that of the catalyst. There is some doubt concerning how the a. c. conducting resin will effect the point-to-point contact resistance of the electro-catalyst in its compressed surface layer.

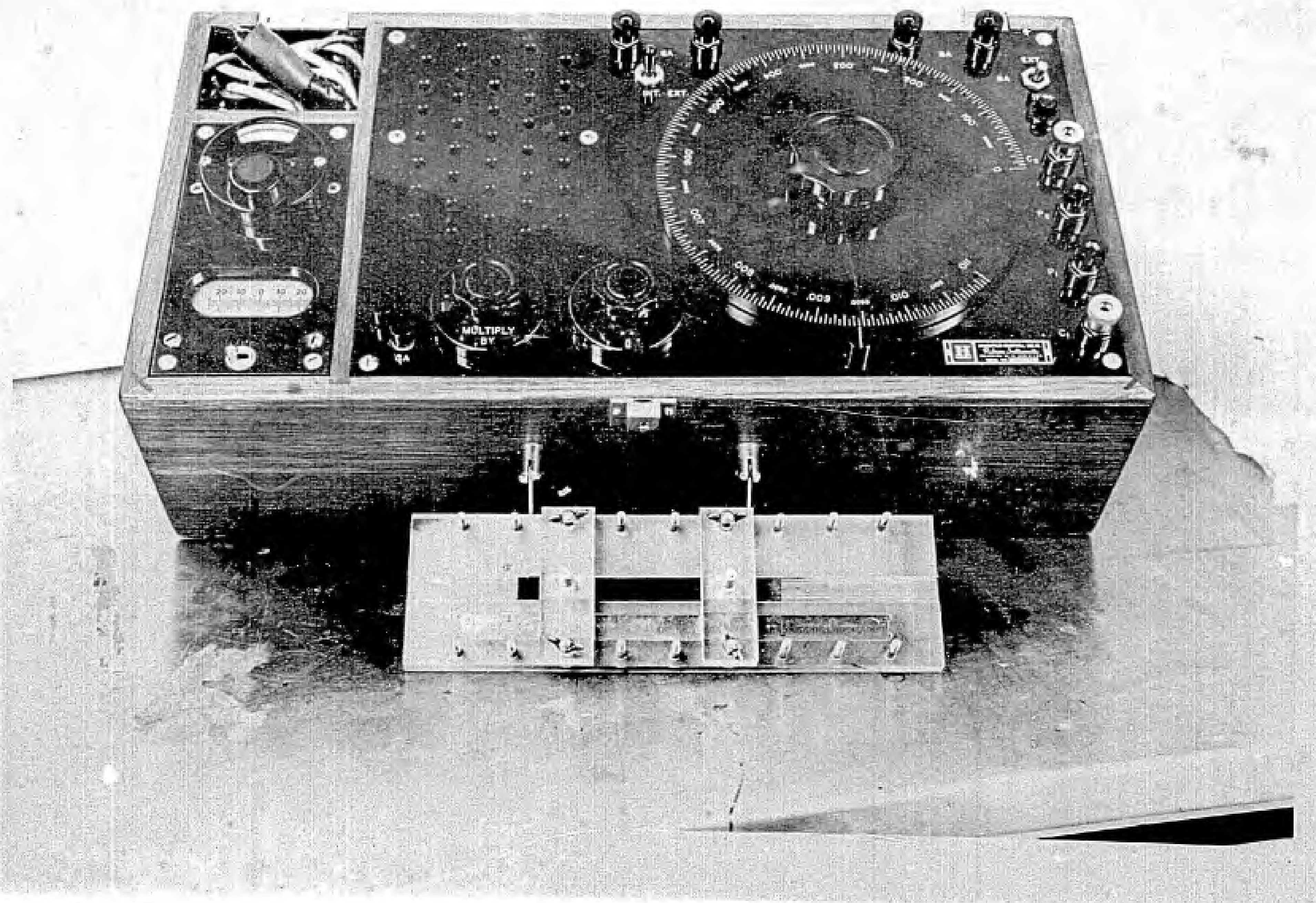

AAT 8223

2. A d. c. measurement on the other hand polarizes the electrode reactions to an extremely high resistance and measures only the electron carrying or catalyst component. This resin polarization often takes over ten minutes using the low currents available in the sensitive laboratory d. c. bridge.

The d. c. bridge was used because of its greater accuracy as well as the fact that the values obtained are less affected by any resin present in the catalyst layer.

A rule graduated in 0.01 inches is incorporated in the pictured apparatus (Photo #3) and with the aid of a magnifying glass the distance between electrodes can be measured to the nearest hundredth of an inch. Steadied-out resistances, where the resin has been polarized, are measured for three or more distances and a plot of distance versus resistance is made (Figure III). The extrapolation of this plot through zero distance indicates the average contact resistance as the resistance-axis intercept, and the slope of the straight line indicates resistance per unit length. Also the width of the strip is known and the thickness can be measured by microsectioning a cross section of a cell and measuring it under 100 X magnification. For the standard catalyst loading (0.0375 gr. catalyst A per square inch on the hydrogen side and 0.0375 gr. catalyst A plus 0.0375 gr. catalyst B on the oxygen side), the resistances obtained from Figure III are 0.45 ohms/square and 0.39 ohms/square respectively. The microsection (Figure IIIA) shows the hydrogen catalyst to be approximately 0.003 cm. thick and the oxygen catalyst to be approximately 0.006 cm. thick.

Thus ρ = $R \times \frac{A}{\ell}$

where A = side of square x thickness
ℓ = side of square
ρ = ohms/square x thickness
hydrogen = 1.4×10^{-3} ohm cm
oxygen = 2.3×10^{-3} ohm cm

Since the cited microsection thicknesses are only point volues, determined inaccurately, the electro-catalyst layer resistance can be expressed more accurately in terms of ohms per "square" -- a specific resistance divided by an unknown thickness dimension. The unknown thickness is related to the amount of catalyst loading used. In the cited cases,

$(\rho/t)_{\text{hydrogen}}$ = 0.45 ohms per "square"
$(\rho/t)_{\text{oxygen}}$ = 0.39 ohms per "square"

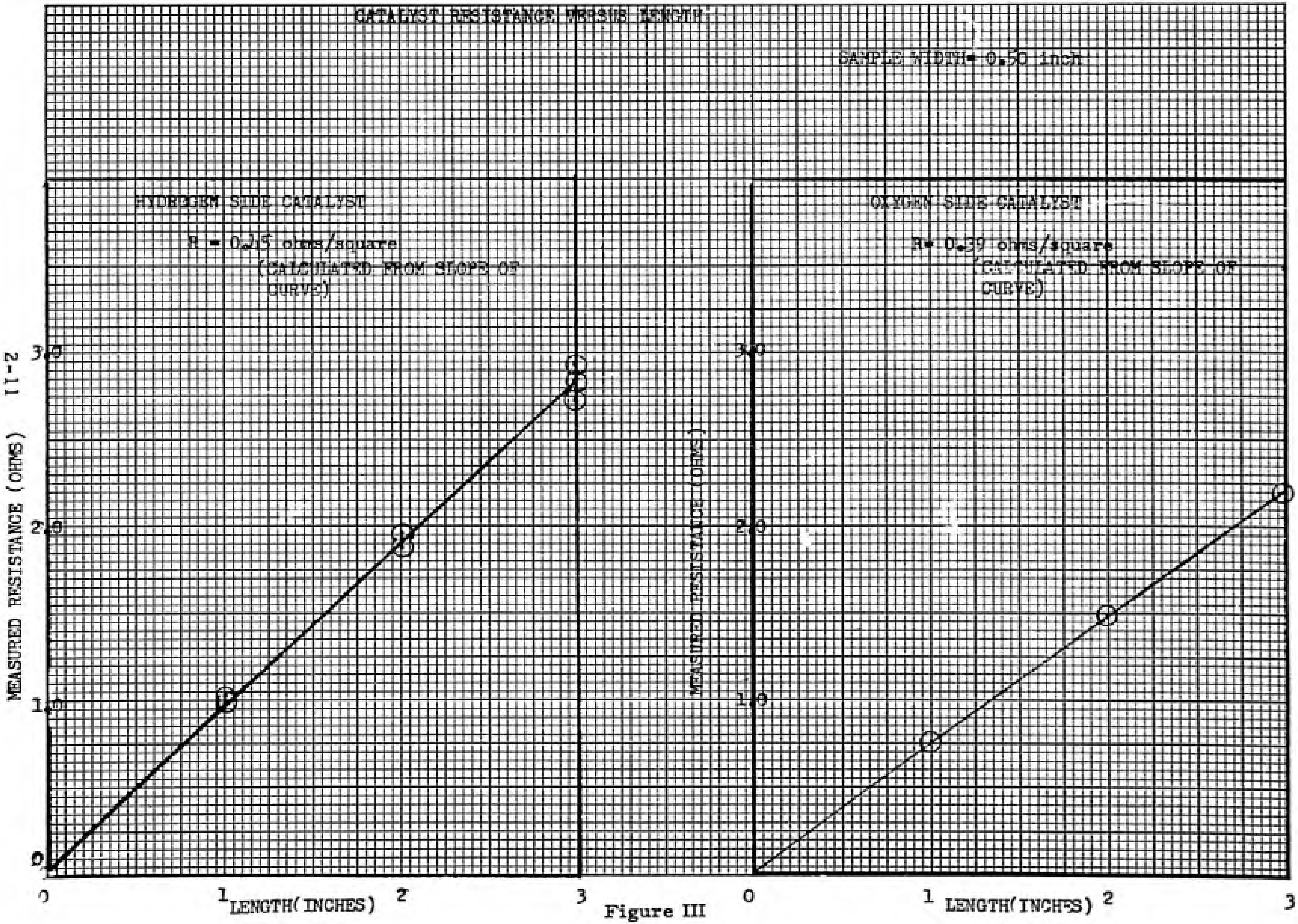
CATALYST RESISTANCE VERSUS LENGTH
SAMPLE WIDTH= 0.50 inch
HYDROGEN SIDE CATALYST
R = 0.45 ohms/square
(CALCULATED FROM SLOPE OF CURVE)
OXYGEN SIDE CATALYST
R= 0.39 ohms/square
(CALCULATED FROM SLOPE OF CURVE)
MEASURED RESISTANCE (OHMS)
0
1.0
2.0
3.0
LENGTH(INCHES)
0
1
2
3

Figure III

MICROSECTION OF CELL
(PHOTOGRAPHED UNDER 100X MAGNIFICATION)

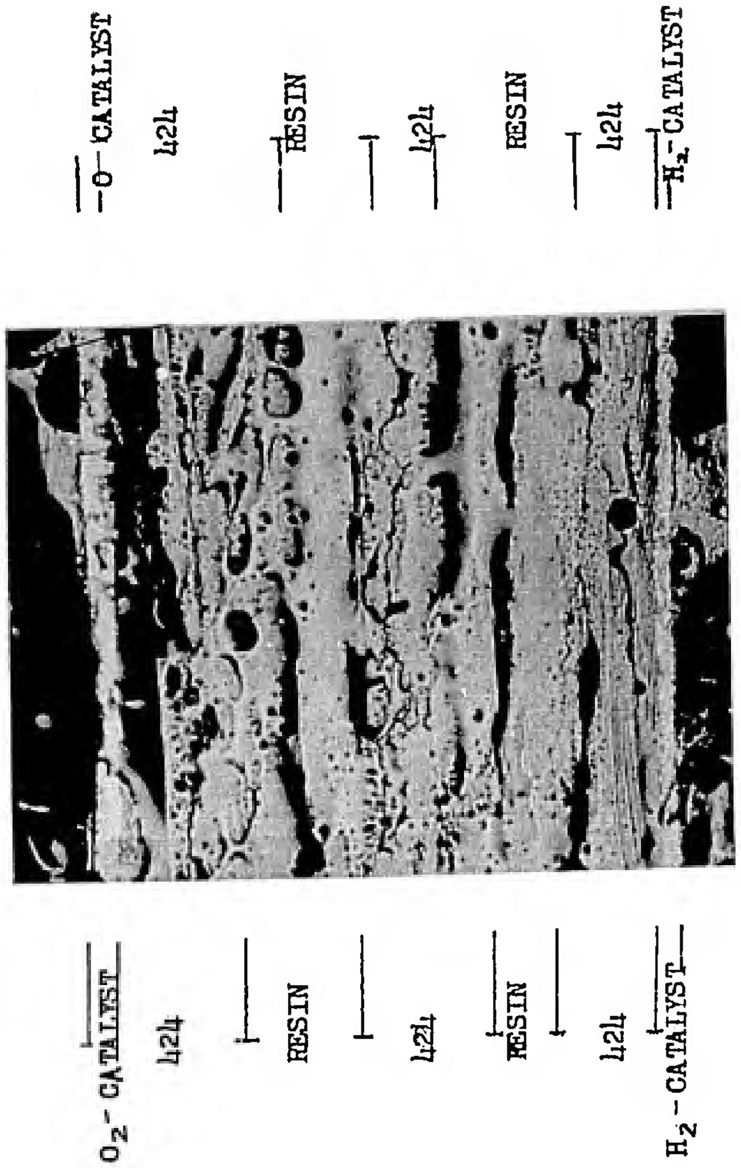

Figure III-A

2.2.2 RESIN RESISTIVITY MEASUREMENT

The method for measuring pure resin resistance is quite similar to the diminishing cell length principle used to measure catalyst resistance. A slab of resin is cured in the form of a rectangular block having the dimensions of 2" x 0.5" x 0.1". Three platinum screens are "cured" within the slab along with the resin as shown in Figure IV. After the slab has been leached sufficiently in distilled water to remove the free sulfuric acid, an a.c. resistance measurement is made between sets of screens using a General Radio Impedance Bridge. Note: d.c. measurement cannot be used as this causes polarization of the electrode reaction. The distance between the screens is carefully measured and a plot of distance versus resistance made by means of which the average contact resistance may be obtained by extrapolation. In this case the screens are so well imbedded in the resin that the contact resistance is usually found to be very near zero. The slope of the curve gives resistance per unit length which multiplied by area (thickness times width) given specific resistivity of the unreinforced or pure ion-exchange resin. A typical curve with sample calculations is shown in Figure V.

The specific resistivity, ρ, may be multiplied by a cell thickness and divided by a selected cell area to convert it to the ohmic resistance of the resin element in the cell. The table below shows typical resistivities obtained from three slabs of standard resin and one slab each of three modified resins. These resistivities were obtained at 100% RH and 25°C. In general, the resin conductivity (reciprocal of resistivity) is most sensitive to relative humidity. Previous investigations have noted resin conductivity decreasing by a factor of ten when the relative humidity drops from 100% to 50%.

Resin	ρ (ohm cm)	Ohmic Resistance of a Pure Resin 0.030" thick cell (ohm-cm^2)
PFR-6	22	1.7
PFR-10A	49	3.7
SB	11	0.85
Standard	14	1.1
Standard	13	1.0
Standard	14	1.1

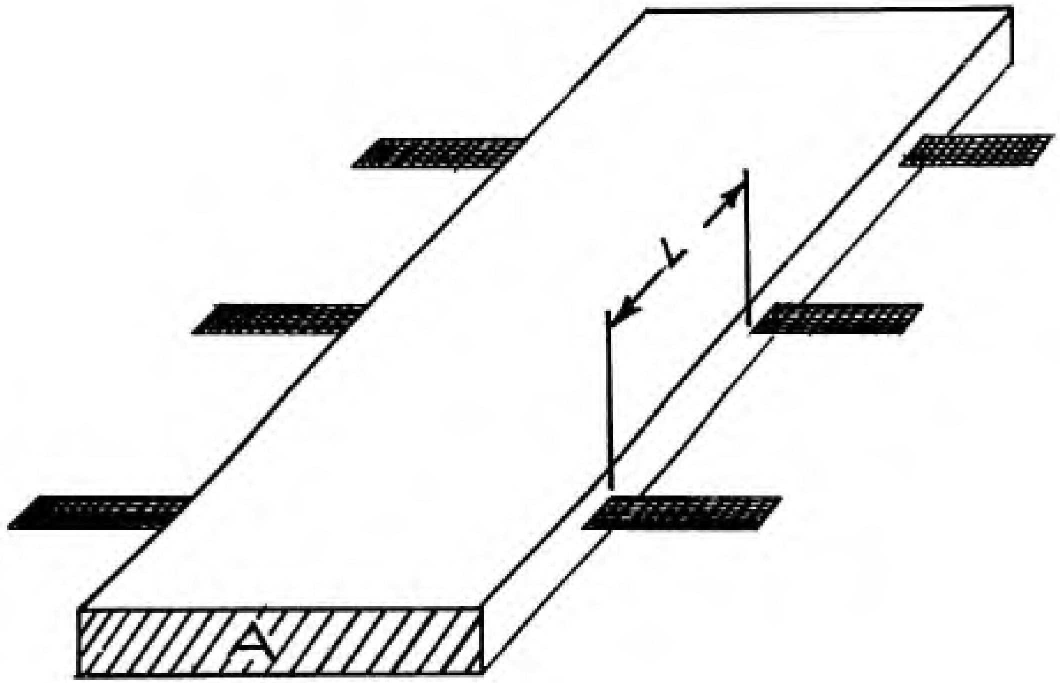

Fig IV RESIN SLAB WITH PLATINUM SCREENS FOR RESISTANCE MEASUREMENT

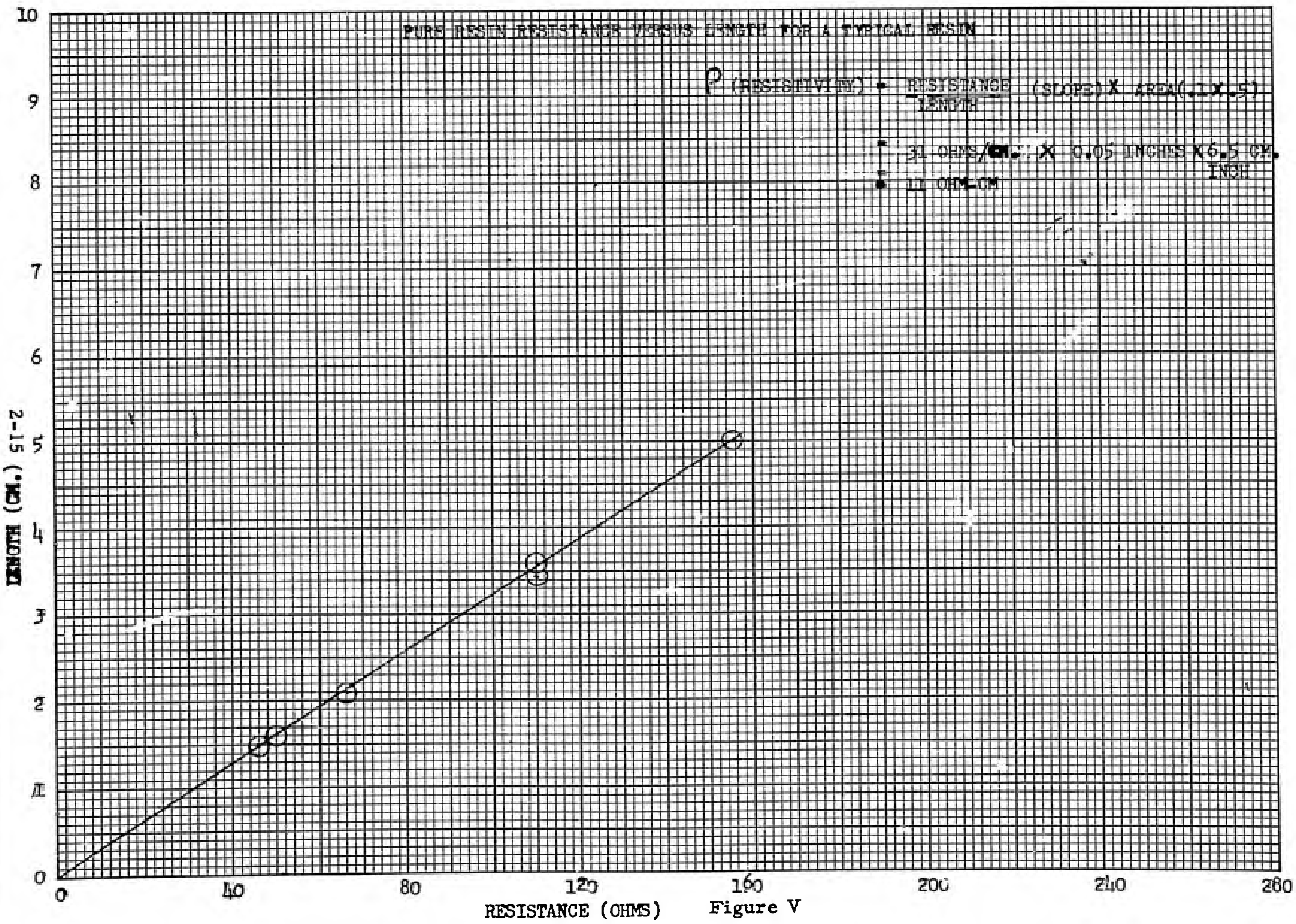

PURE RESIN RESISTANCE VERSUS LENGTH FOR A TYPICAL RESIN
ρ (RESISTIVITY) = RESISTANCE / LENGTH (SLOPE) X AREA(.1 X .5)
= 31 OHMS/CM. X 0.05 INCHES X 6.5 CM./INCH
= 11 OHM-CM
LENGTH (CM.) 2-15
0
1
2
3
4
5
6
7
8
9
10
0
40
80
120
160
200
240
280
RESISTANCE (OHMS)

Figure V

2.2.3 MEMBRANE RESISTANCE INDEPENDENT OF ELECTRO-CATALYST RESISTANCE

An a.c. impedance bridge is used to measure the resistance of a 3.0" x 3.0" cell. The electrodes used for this measurement are gold-plated brass plates with 3.0" x 3.0" contacting faces. The electrodes are tightened down until further tightening does not change the cell resistance. This resistance measurement is independent of the catalyst resistance for the gold-plated electrodes offer a large conducting path in parallel to the catalyst thus eliminating the catalyst resistance in the plane parallel to the cell surface. In the plane perpendicular to the surface:

$$R = \rho \times \frac{\ell}{A} \qquad \text{where } \ell = 0.003 + 0.006^{*}\text{cm}$$

$$A = 40.0 \text{ cm}^2$$

$$\rho = 10^{-3*}$$

$$R = \frac{10^{-3} \times 10^{-2}}{4 \times 10^{2}}$$

$$R \quad 10^{-7} \text{ ohms (negligible)}$$

Thus, the resistance measured in this manner is that of the membrane (resin and cloth) plus the contact resistance (fixture resistance can be shown to be negligible.)

Before the resistance obtained in this manner can be compared to the Kordesch-Marko resistance and the pure membrane (cloth and resin) resistance can be found, an approximate evaluation of the contact resistance must be made. It is believed at present that the contact resistance is inversely proportional to contact area as well as increasing pressure up to some critical pressure.

* These values are derived in Section B.

2.3 FUTURE WORK

A third method of determining cell ohmic resistance involves driving a cell with a steady direct-current source and measuring the potential drop across the cell for a known current when both sides of the ion-exchange fuel cell are exposed to pure moist hydrogen gas. For this scheme to work, both electrocatalyst layers must not polarize to a noticeable extent -- both the forward and the reverse hydrogen electrodes must be nearly "reversible". Preliminary evidence indicates this situation is nearly the case. Therefore, it is presently planned to accomplish these measurements during the next two-month period (October-November) so that a comparison with the other two methods can be made. Using the experimental setup with current densities over 10 ma/cm^2, some idea may be found concerning the current density needed to make hydrogen electro-catalysis polarization become noticeable.

Second, a set of experiments will be designed to evaluate contact resistance present in the ion-exchange fuel-cell assemblies where current collectors are used.

Third, during the next reporting period, a start will be made in setting up a mathematical model of the ohmic resistance part of the fuel cell. When perfected, this model will estimate the total ohmic resistance of a cell when specific resistances of each component and the cell assembly configuration is specified. Also the model will allow assignment as percents of the total resistance, the resistance due to each component.

3.0 TASK 1B - MINIMIZATION OF ELECTROLYTIC LOSSES

A preliminary method was devised to correlate the cell construction with total cell ohmic resistance. This method involves the calculation of individual cloth-resin resistance and summing these as in a series-circuit to obtain a total resistance.

3.1 INVESTIGATE RESIN FORMULATIONS

The investigation on this work problem will be initiated at a later date.

3.2 APPROXIMATE CALCULATION OF IMPREGNATED-CLOTH RESISTANCES

Using cells made of various constructions of different fabrics, impregnated with the same resin, one can estimate the separate impregnated fabric resistances. The resistances are assumed to be in series with negligible contact and catalyst resistance. This assumption is probably only approximate, and suitable corrections will be made as soon as reliable values of these resistances are obtained. Also the proper pure-resin resistance is used if the cell is thicker than the sum of the cloth thickness. For example, in the sketch in Figure VI, the total resistance of the cell will be

$$R_m = 2(R\ \text{resin})^* + (R\ \text{cloth}\ 1) + (R\ \text{cloth}\ 2) + \underline{\text{nil}}\ (\text{catalyst and contact resist})$$

If the overall thickness of the cell is equal to the sum of the individual cloth thicknesses, then it is assumed that there is not excess resin. If the overall cell thickness is less than the sum of the cloths, then the resilient cloth is assumed to compress but to have no change in resistance. The resistance will decrease with the thickness and will be compensated by an increase in cloth density. This last assumption is valid only for slight cloth compressions.

Using Cells 11, 44, and 57, whose overall resistances were measured by the large flat current-collectors, simultaneous equations were set up to find the separate resistances under the assumption previously cited.

* In Figure VI the excess resin is assumed to exist as two equal stack layers, one on each side.

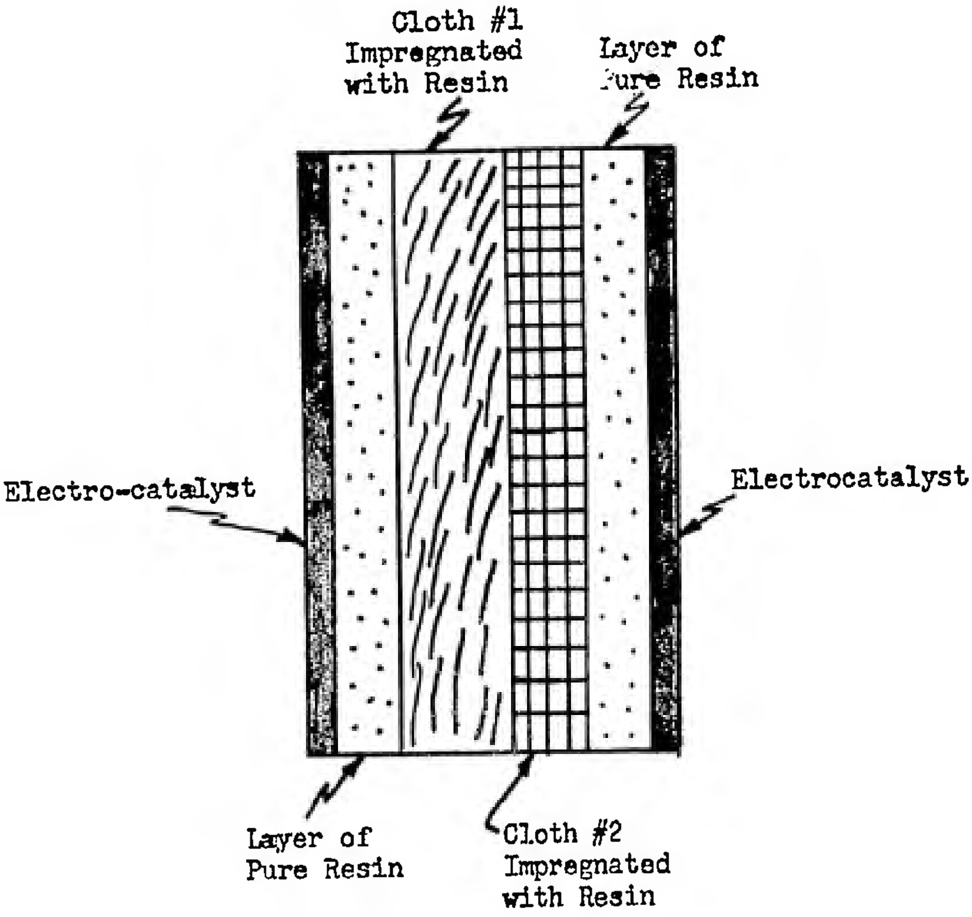

FIG VI TYPICAL VIEW OF CROSS SECTION OF FUEL CELL

Cell	Measured Resistance	Thickness	Construction
11	1.75 ohm cm^2	.019 inch	234 (.020 thick) *
44	2.16 ohm cm^2	.021 inch	DN (.005 thick 3 ply) **
57	3.39 ohm cm^2	.029 inch	DN/234/DN **

Pure resin resistance was found to be 0.0558 ohm-cm^2 per mil.

Thus, the following equations can be written:

$R_{234} = 1.75$ ohm-cm^2 Cell 11

$3\ R_{DN} + 6(.0558) = 2.16$ Cell 44

$2\ R_{DN} + R_{234} = 3.39$ Cell 57

$R_{DN} = 0.610$ Cell 44

* Type of cloth (Webril)
** Dacron-Ninon

Checking by Cell 57

Calculation vs Observed
1.22 + 1.75 vs 3.39
3.00 vs 3.4

About ten per cent agreement which is considered good with the assumptions that have been made. In summary of this method, the following table of approximate resistances associated with resin impregnated cloths is presented.

Cloth	Cloth Construction	Cloth Weight	Cloth Thickness	Resistance of Impregnated Cloth Element
234	non-woven dynel	.055 gr/in^2	.020 inch	1.75 ohm-cm^2
424	non-woven dynel	.055 gr/in^2	.006 inch	2.58 ohm-cm^2
DN	woven dacron	.031 gr/in^2	.005 inch	0.610 ohm-cm^2
1-1/2 234	non-woven dynel	.089 gr/in^2	.024 inch	2.06 ohm-cm^2

From the above data, the resistances of all cells tested were calculated and compared to measured values in Table III.

TABLE III - COMPARISON BETWEEN SIMPLE CELL MODEL & EXPERIMENT

Cell No.	Construction	Thickness (inch)	Excess Resin Resistance (ohm-cm^2)	Impregnated Cloth Resistance			Calculated Resistance (ohm-cm^2)	Measured Resistance (ohm-cm^2)	Percent Deviation
				Ply 1	Ply 2	Ply 3			
9	234	.035	0.84	1.75	--	--	2.59	2.47	+ 4.9%
10	234	.029	0.50	1.75	--	--	2.25	2.06	+ 9.2%
11	234	.019	--	1.75	--	--	1.75	1.75	--
12	234	.023	0.17	1.75	--	--	1.92	1.75	+ 10%
13	3 ply 424	.017	--	2.58	2.58	2.58	7.74	8.00	- 3.3%
44	3 ply DN	.021	0.34	0.61	0.61	0.61	2.17	2.16	+ 0.5%
56	DN/234/DN	.024	--	0.61	1.75	0.61	2.97	2.67	+ 11.2%
57	DN/234/DN	.029	--	0.61	1.75	0.61	2.97	3.39	- 14.1%
58	DN/234/DN	.019	--	0.61	1.75	0.61	2.97	2.37	+ 20.3%
59	234	.028	0.45	1.75	--	--	2.20	2.16	+ 1.8%
60	234	.022	0.01	1.75	--	--	1.76	1.85	- 4.9%
61	234	.018	--	1.75	--	--	1.75	1.85	- 5.4%
83	DN/234/DN	.030	--	0.61	1.75	0.61	2.97	2.75	+ 7.4%
84	424/234	.030	0.22	2.58	1.75	--	4.55	5.25	- 13.4%
BP	424/234/424	.030	--	2.58	1.75	2.58	6.91	6.90	--
87	2 ply 1 1/2 234	.032	--	2.06	2.06	--	4.12	4.22	- 2.4%
88	2 ply 234	.033	--	1.75	1.75	--	3.50	2.75	+ 27.0%
89	234/DN/234	.032	--	1.75	0.61	0.75	4.11	3.00	+ 37.0%
90	DN/1 1/2 234/DN	.029	--	0.61	2.06	0.61	3.28	3.00	+ 11.0%
91	DN/1 1/2 234/DN	.029	--	0.61	2.06	0.61	3.28	3.40	- 3.4%
92	1 1/2 234	.019	--	2.06	--	--	2.06	2.37	- 18%
94	1 1/2 234	.021	--	2.06	--	--	2.06	2.06	--
95	DN/234/DN	.025	--	0.61	1.75	0.61	2.97	2.58	+ 15.1%

Table III indicates that present reliability of this method in correlating resin-cloth resistances with overall cell resistance. At this date, this method and the data used in applying it are by no means ultimate in their reliability and accuracy. The table does indicate that with more accurate data and a better understanding of what actually happens and how to allow for it, this method will enable a reliable prediction of actual cell resistance once the basic reinforcement is characterized.

3.3 EVALUATE REINFORCING MATERIALS

The work involved in this problem will be done at a later date.

4.0 TASK 1C - MINIMIZATION OF ELECTRONIC LOSSES

The work on this problem will be done at a later date.

5.0 TASK II - INTERNAL GENERATION AND STORAGE OF HYDROGEN FUEL

Work to be accomplished at a later date.

5.1 PALLADIUM AND OTHER ABSORBENTS

This work will be accomplished by the General Electric Heavy Military Electronics Department at Syracuse, New York and will be reported under separate cover by the above department.

5.2 ELECTROLYSIS BY ION MEMBRANE FUEL CELLS

Work to be accomplished at a later date.

6.0 TASK III - EXTERNAL GENERATION AND STORAGE OF HYDROGEN AND OXYGEN

6.1 ELECTROLYTIC METHODS

6.2 CHEMICAL METHODS

All of the work in Task III, Section 6.0 will be accomplished at a later date.

7.0 APPENDIX

A. Photographs

  1. Kordesch-Marko Bridge

  2. Apparatus for Measuring Membrane Resistance

    a. Independent of Electro-Catalyst

    b. Including Electro-Catalyst

B. Fuel Cell Development

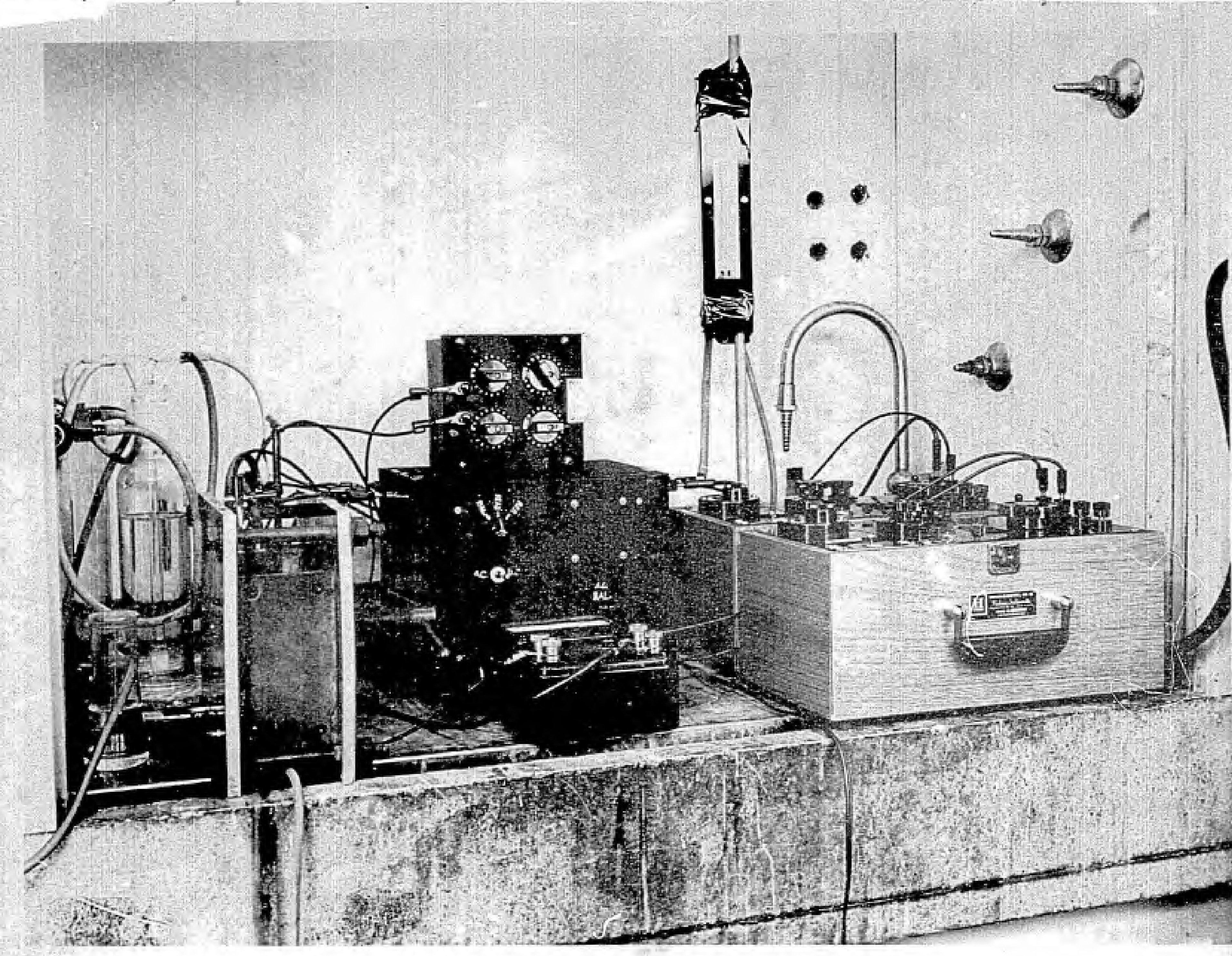

NOT REPRODUCIBLE

AAT 8222

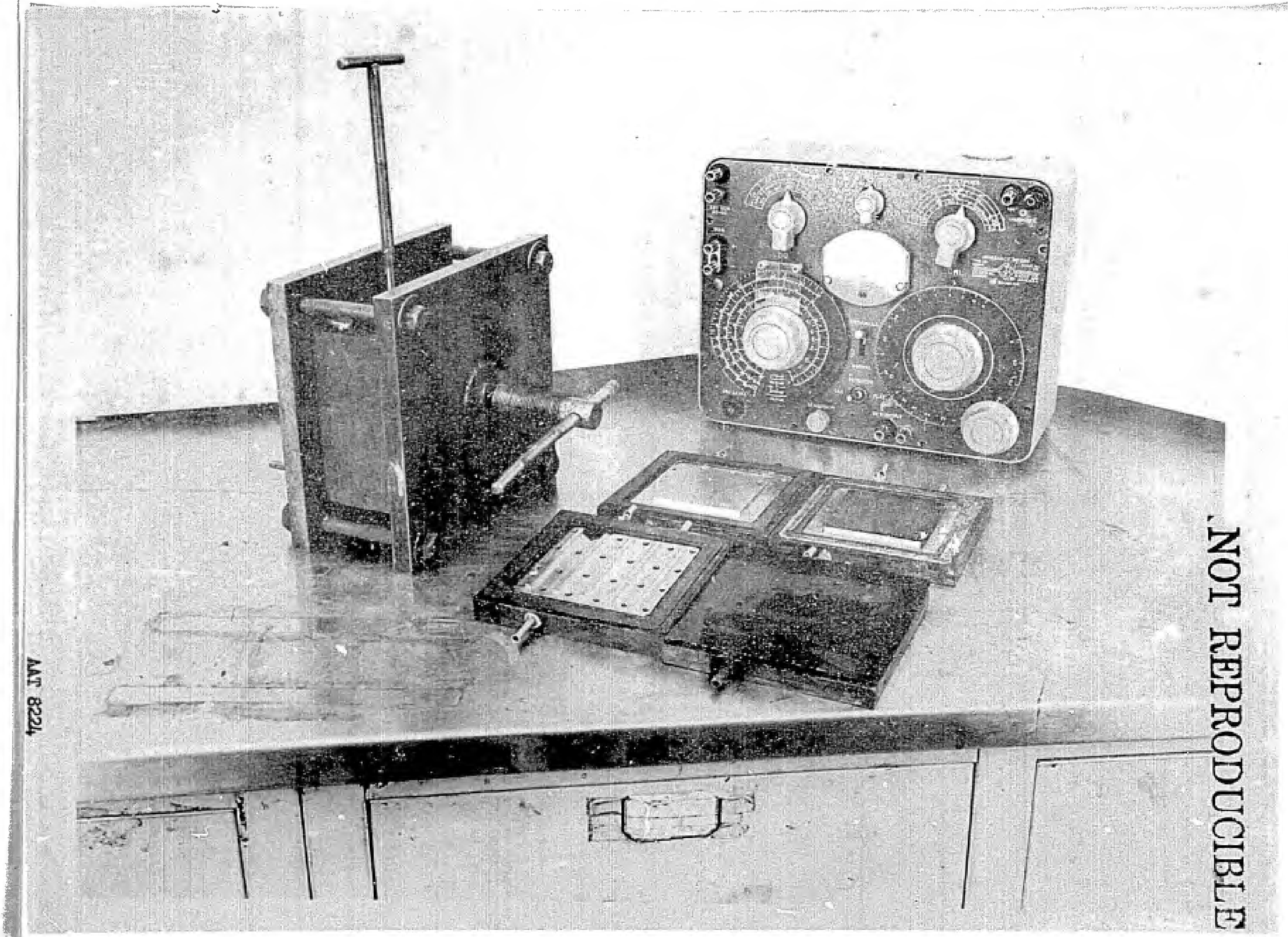

NOT REPRODUCIBLE

AAT 8224

BLANK PAGE

FUEL CELL DEVELOPMENT

ION EXCHANGE MEMBRANE FUEL CELL

by

L. W. NIEDRACH

1959

Progress Report from General Electric

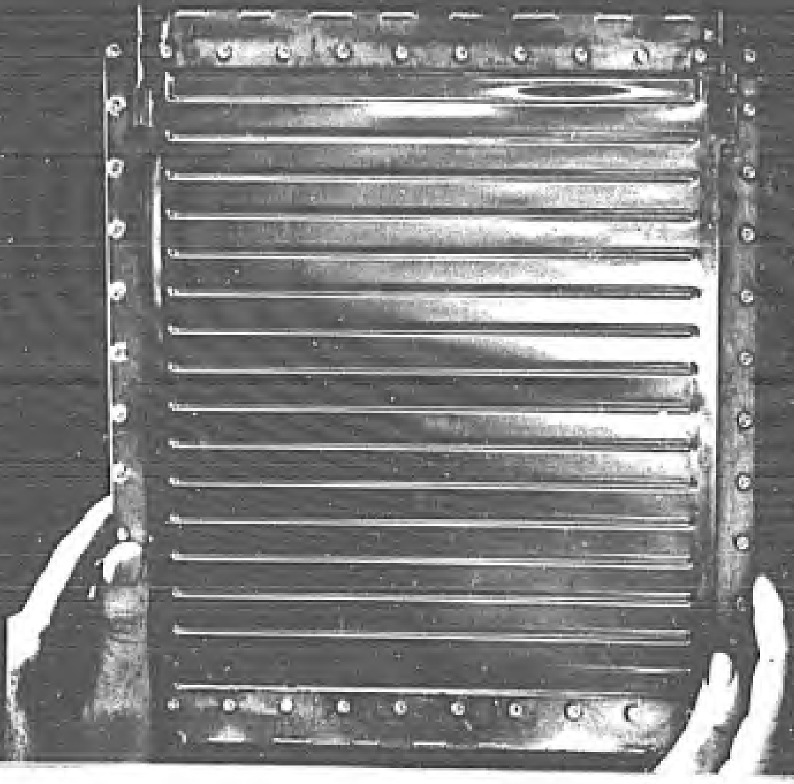

ION EXCHANGE MEMBRANE FUEL CELL BATTERIES

by

E. A. OSTER

1960

The two papers contained in this pamphlet review the development and present status of General Electric's ion-membrane fuel cell and fuel cell batteries.

These papers were presented approximately one year apart and indicate the rapid development activity that took place during a 12-month period.

In the Spring of 1959, fuel cells were a new development at the General Electric Research Laboratory. Output was measured in milliwatts.

In the Spring of 1960, at the General Electric Aircraft Accessory Turbine Department significant progress had been made in fuel cell development: their cost had been reduced fifty-fold and their size had been increased fifty-fold with corresponding increase in output.

The Ion Exchange Membrane Fuel Cell

by **Dr. L. W. Niedrach**
General Electric Company — Research Laboratory

For Thirteenth Power Sources Conference
Atlantic City, New Jersey — April 29, 1959

The fuel cell that is to be described is a relative newcomer to the field although W. T. Grubb reported briefly on this type at the Battery Conference in 1957. It is the purpose of this paper to present results obtained using cells incorporating features which greatly improve the operating characteristics over those previously reported.

The principles upon which the membrane cell is based are, of course, common to all such devices. The novelty of our cell is in the use of an ion exchange membrane as the electrolyte. In addition, our cell is unusual in that it employs an acidic electrolyte — a cation exchange resin in its hydrogen form. Anion exchange resins in their hydroxyl form may be employed, but our greatest activity has been with cation resins in their hydrogen form.

Use of the acidic electrolyte results in some fundamental differences from cells employing potassium hydroxide or other caustic electrolytes. Thus, in our cell hydrogen ion, rather than hydroxyl, is the charge carrier. This results in mass transport through the electrolyte from the hydrogen to the oxygen electrode where the product, water, is formed. The formation of the water at the oxygen electrode is advantageous, particularly because the acidic electrolyte permits direct operation on untreated air. The cell can therefore be operated with an exposed air electrode from which the water can be removed by controlled evaporation. If desired, flowing air can be pumped through the cell to accomplish the same net effect.

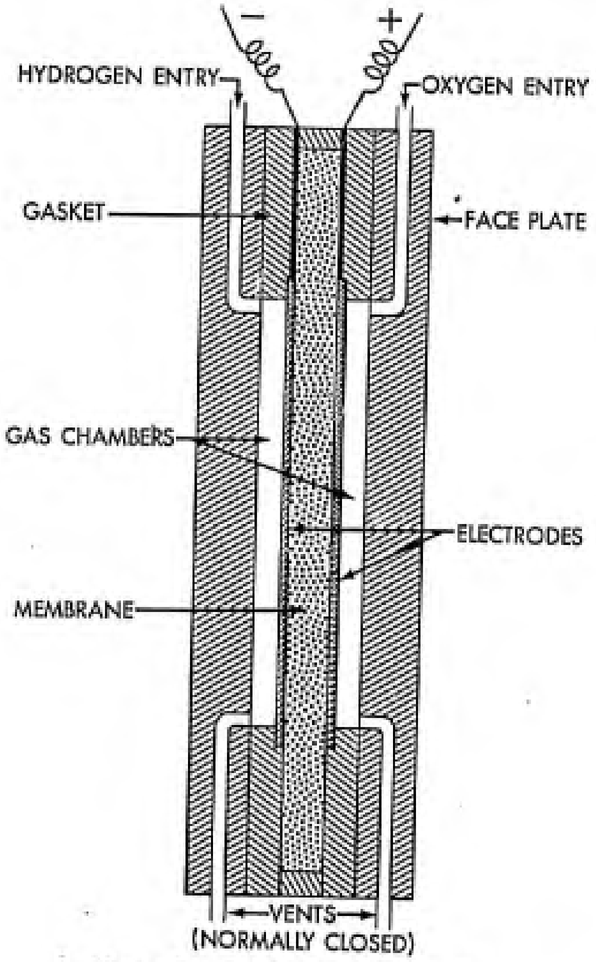

Figure 1. Cell Structure Schematic

A schematic diagram of a membrane fuel cell is shown in Figure 1. Heart of the unit is the ion exchange membrane electrolyte with the two electrodes against its opposite faces.

In the completed cell assembly the membrane also serves to delineate the hydrogen and oxygen chambers. As indicated the cells are normally operated on static gases — usually under a few *inches* of pressure. Commercially available electrolytic hydrogen has proved highly satisfactory. In contrast, the small amount of nitrogen impurity in commercial oxygen has proved to be a nuisance during operation on a static head of gas. This nitrogen tends to concentrate in the small volumes of our gas chambers and in time causes concentra-

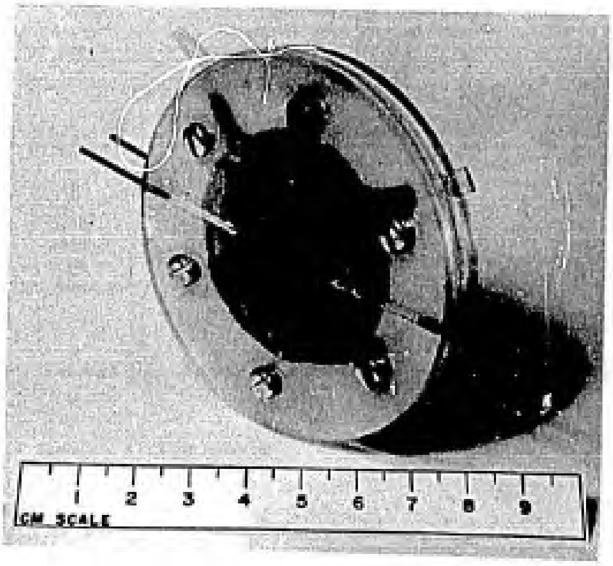

Figure 2. Ion-exchange membrane fuel cell showing plastic housing, tubes for gas inlets and outlets, and metal screen tabs for electrode connections.

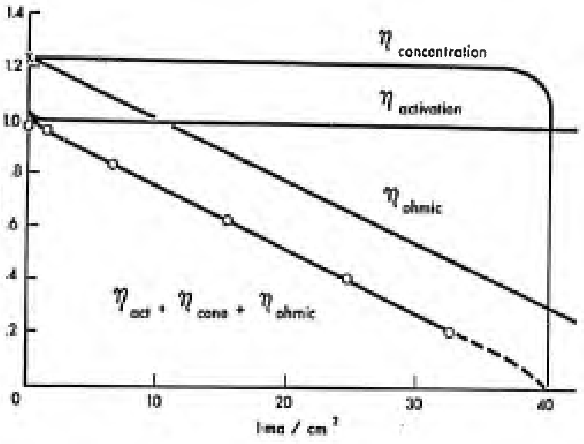

Figure 3. Polarization Curves

tion polarization. Although a few seconds' purge of the oxygen chamber restores the cell to normal operation, we have found that the substitution of electrolytic oxygen minimizes the problem from such impurities. We mention this as a detail warranting consideration for future applications.

In all of the work to date, operation has been at room temperature and the aqueous product is in the liquid form. The water drains to the bottom of the oxygen chamber and then flows from the cell through the vent line which is closed by a simple water seal.

A picture of one of our experimental cells is shown in Figure 2. The compactness of the structure is quite evident as is the possibility of construction from light-weight polymeric materials.

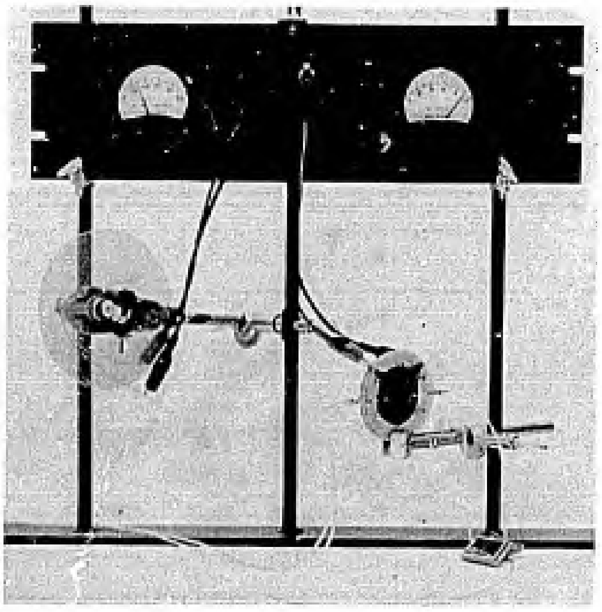

Figure 4. Operating Unit. Fuel Cell (right) powers small electric motor (left).

A typical performance curve for an ion exchange membrane cell is shown in Figure 3. In common with other gas cells the cumulative effects of a number of types of polarization are in evidence. Activation polarization is important at low current densities. The linear region is at least in part associated with ohmic drop. Finally at high current densities, or when nitrogen impurities accumulate in the oxygen chamber, diffusion control becomes important. The contributions from these independent sources are indicated schematically in the figure.

Our units have a very low stacking factor since the cell thickness is small, as is that of the associated gas chambers. As a result, when one thinks in terms of power per unit volume or weight, the performance of our cells is very attractive. Thus we have calculated power densities of the order of 1 to 2 kw per cubic foot on the basis of present performance data.

A number of our cells have now been operating continuously and satisfactorily for periods upwards of 75 days, and the tests are continuing. Most of this operation has been at the low current density end of the curve — 3 ma/cm², but in some cases operation at about 30 ma/²cm for several days has been interspersed with the low density periods. One of these cells has been driving the small motor shown in Figure 4 for over 100 days.

Table I
Characteristics of the Membrane Fuel Cell Shown Operating in Figure 4

Thickness of Electrolyte	0.6 mm
Electrode Area	11.4 cm²
Performance Data:	
As Operating	
Voltage	0.9 v
Current	0.03 amp.
Power	0.027 watt
Efficiency (Thermal)*	62%

*Based on ΔH for the reaction:
H_2 (gas) + ½ O_2 (gas) → H_2O (liquid)

The characteristics of the cell shown in operation are summarized in Table 1. It should be noted that the thermal efficiency indicated is based on ΔH for the reaction of *gaseous* hydrogen and oxygen to form *liquid* water. Current efficiency of 100 per cent has been assumed, and preliminary experiments justify such an assumption.

The ability of our cells to operate on air has been shown by the continuous operation of two cells having their anodes exposed to static hydrogen and their cathodes to air. One of these cells has been in continuous operation for over 75 days.

As a result of the preliminary tests outlined above, it is felt that the ion exchange membrane fuel cell has a number of noteworthy features. These include:

1. The use of the solid polymer electrolyte results in an extremely compact unit cell structure.
2. The cell can be operated on static heads of gas.
3. There are no moving parts.
4. The acidic type electrolyte permits operation on gases containing carbon dioxide, e.g. air or diluted hydrogen such as might be obtained by reacting fossil fuels with water.
5. No close tolerances are required in the construction of the cells nor should they be necessary in the assembly of batteries.

Acknowledgement

I am grateful to W. T. Grubb, M. M. Safford, J. R. Ladd, and M. C. Agens for much helpful discussion during the course of this work.

Ion-Exchange-Membrane Fuel-Cell Batteries

by Dr. E. A. Oster

General Electric Company — Aircraft Accessory Turbine Department

For Fourteenth Power Sources Conference
Atlantic City, New Jersey — May 18, 1960

Last year at the Thirteenth Power Sources Conference, L. W. Niedrach reported on improvements in the ion-exchange fuel-cell which indicated this device[1] was a practical source of power for special applications. This paper describes the development of this cell during the past year for air-breathing portable ground-power units.

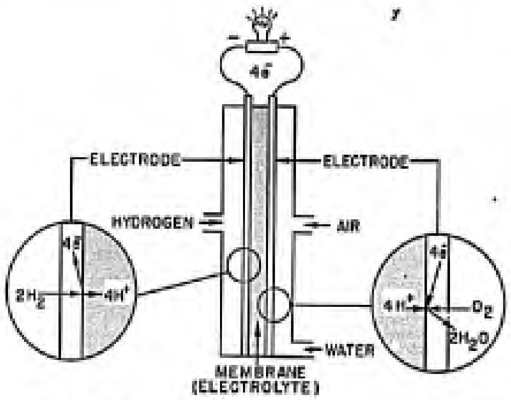

Figure 1. Cell structure schematic showing relationship of electrolyte to electrodes. Not to scale.

The G-E ion-exchange-membrane fuel-cell to be discussed consists of a cationic reinforced-resin membrane about 0.8 mm thick having a thin layer of catalyst on each side. As shown in the schematic diagram of a membrane fuel cell in Figure 1, on one side of the membrane, hydrogen gas is adsorbed on the catalyst where it can be stripped of one electron per hydrogen atom. The resultant hydrogen ions diffuse through the hydrated cationic resin while the freed electrons flow along the electrically-conducting catalyst to the nearest pickup contact that feeds the minus terminal of the cell. On the other side of the membrane, which separates the gases, the oxygen in the air is adsorbed on the catalyst. Here a three-way reaction of the hydrated hydrogen ions from the cationic resin, the electrons from the electrically-conductive catalyst, and the adsorbed oxygen yield water as the product. The water formed on the oxygen side collects at the cell bottom or is evaporated by the convecting air. The oxygen catalyst is furnished electrons through electrical pickups at the cell's positive terminal.

Figure 2 compares the small cell reported last year and the present membrane now being pro-

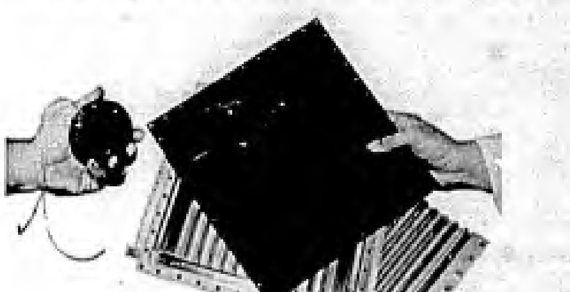

Figure 2. Scale-up of Ion-Exchange Fuel Cell during 1959: early Research Laboratory unit at left; 90 sq. in. air-breathing membrane, at right, with two electrical pickups.

---

[1] U.S. Patent No. 2,913,511, W. T. Grubb; assigned to General Electric Co., 1959

duced in quantity by the Aircraft Accessory Turbine Department in Lynn, Massachusetts. The size difference represents an area scale-up of fifty times.

A series of these scaled-up cells powers an air-breathing portable ground-power unit being developed under contract with the Navy Bureau of Ships and the Army Signal Corps. Figure 3 shows the end view of the portable unit under development with an inset showing how this unit will be carried. When completely developed this portable back-pack unit will furnish 200 watts of DC power for 14 hours of operation. Subsequent 14-hr periods will be obtained by plugging in a new 7-lb fuel canister containing a 4.5-lb chemical system that generates the hydrogen fuel.

Figure 3. Mock-up of 200-watt unit. Hydrogen accumulator is at right of replaceable fuel canister. Inset indicates size and carrying position.

In Figure 4 are two polarization curves obtained for large-sized cells running near room-temperature ambient. The hydrogen-oxygen curve is representative of operation on pure gases which are either "dead-headed" or slowly recirculating. The lower curve for hydrogen-air operation is representative of a more defined set of operating conditions for naturally-convecting air. The use of forced-convected air of different inlet-temperatures, humidities, and velocities alters the position of the air-operation curve to some degree.

Before taking up the various irreversibilities of the ion-exchange cell, it would be well to note the effect of membrane temperature on cell operation. Increasing temperature up to about 165F improves cell performance while the cell has a very slight output at −65F. Temperature-cycling an activated membrane does not noticeably change cell performance.

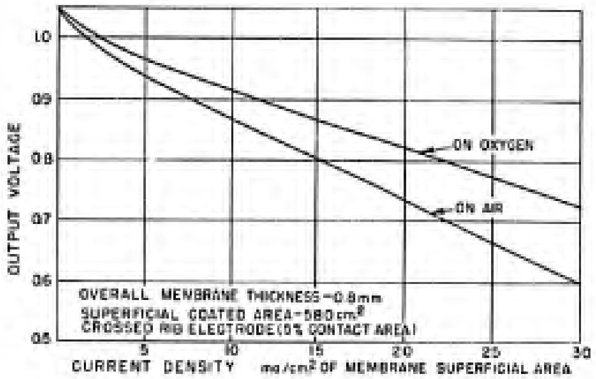

Figure 4. Single-cell polarization curves for ion-exchange fuel cells operating on hydrogen/oxygen and hydrogen/ambient air.

Humidity

Besides pickup contact-resistance and catalyst-layer ohmic losses, the ion-exchange resin generates a loss associated with the flow of hydrated hydrogen ions. The effect of changes in the air's relative humidity on the ohmic and dimensional properties of a standard ion-exchange resin is shown in Figure 5. The air in the illustration is in moisture equilibrium with the resin. Operating cells, in which water and heat are given off, and stored cells, in which near equilibrium exist, both reflect changes in properties and performance consistent with the part played by resin resistance in the total cell irreversibilities. The original properties can be nearly restored by rehumidifying cells — usually done by immersing the cells in water. At other than near 100 percent or 0 percent relative humidity, a double curve of properties versus humidity not unlike a hysteresis loop is found for the first few times a resin is cycled. Sets of curves exist for each general type of resin.

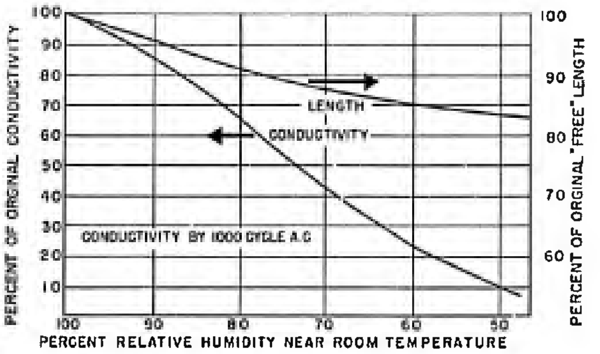

Figure 5. Change in conductivity and unrestrained length of the standard type of ion-exchange resin as flowing air dries it out.

The amount which a given type of ion-exchange membrane wishes to change length may be affected by the amount of cross-linking present in the resin and by the type and amount of fiber-reinforcing present. Cross-linking in resins may be induced by changing the amount of polymer-forming reactants, the use of different chemical additives, or varying curing conditions up to the point where the stiffening of the resin results in a too-low resin-conductivity. Similarly, the amount of reinforcing may be increased up to the point where the resultant membrane loses too much conductivity. It is important to make this reinforcing as isotropic as possible for good reliable performance of this type of cell. Changes in membrane "free-length" may be accommodated by using integrally-bonded flexible membrane mounts and by stressing the membrane.

Changes in membrane properties are minimized by improving the humidity of the air in the boundary layer next to the membrane, when operating on dry hot inlet-air. In 1959 this method of humidifying the boundary layer was accomplished by stringing wicks along the surface of the cell's air side as shown in Figure 6. Water was fed to the wicks to keep these cells wet. When the 200-watt unit is operating on air of less than a 25 percent relative humidity and a "dry-bulb" above room temperature, it is estimated that about one pound of water will be evaporated during each hour of operation. Later experimental evidence was gathered to show that the use of very wet wicks cut down cell performance by as much as 30 percent as compared to operation with dry wicks and more humid air. We are now developing a new method of boundary-layer humidification which has not inhibited cell performance.

The humidity problem outlined above is greatly minimized by operating the cell on hydrogen and oxygen.

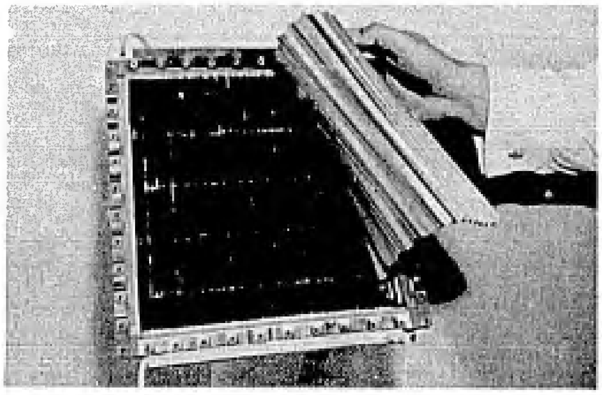

Figure 6. External wicking on air side of membrane allows dry-air operation.

Catalyst

Figure 7 shows the effect on performance of various standard catalyst loadings with pure oxygen. As catalyst loading is changed, also shown are the irreversible effects on cell output-voltage of such variables as catalyst-layer electron-conduction, resin concentration polarization, and catalyst activation polarization. Note that cell performance seems to be optimized with hydrogen-catalyst loadings in the range of 6 to 10 milligrams of catalyst applied per square centimeter of superficial membrane area. This optimization does not occur with the oxygen catalyst as it is usually applied. In this case one would only be limited by

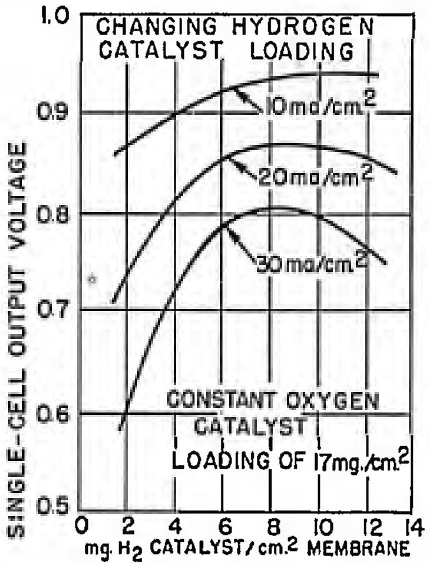

CONDITIONS: 0.63 cm. DIAM. ELECTRICAL PICKUPS SPACED ON 2.54 cm. CENTERS (5% AREA); RUN ON H_2 & PURE O_2; ACID MEMBRANE; ATMOSPHERIC PRESSURE; ROOM TEMPERATURE AMBIENT

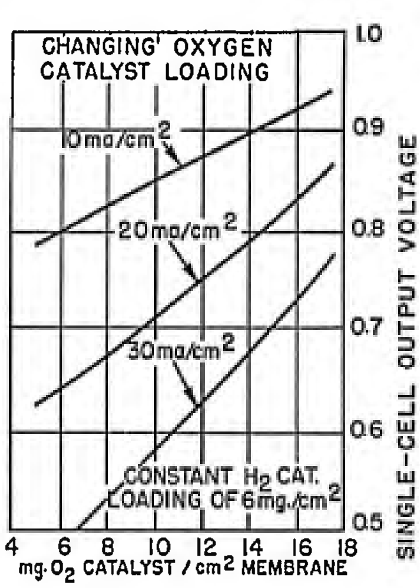

Figure 7. Cell performance with various loadings of standard catalysts.

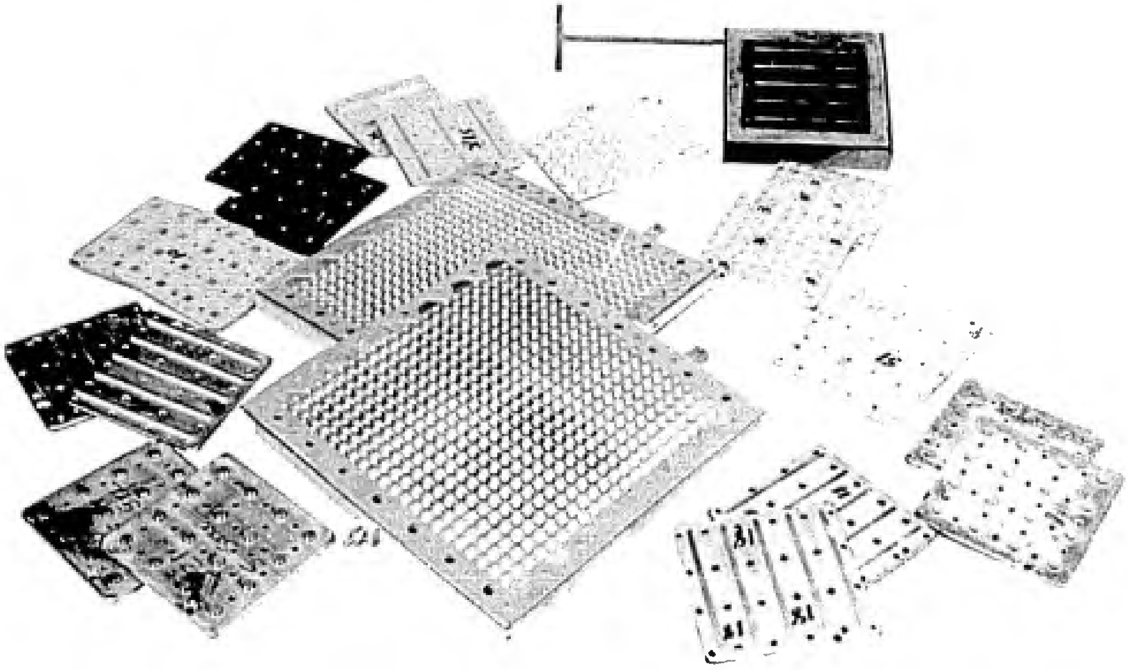

Figure 8. Various electrical-pickup configurations investigated.

the cost consideration and by how much can be made to stay in contact with the ion-exchange resin in an effective manner. The hydrogen and oxygen catalysts reported here are not the same material.

Electrical Pickup

Along with the catalyst-loading optimization, an experimental investigation for electrical-pickup design was conducted. About twenty different pickup configurations were tested with membranes operating on hydrogen and oxygen. Some of the various configurations used in the investigation are shown in Figure 8. Variations in both anode and cathode pickups included circular contacts, square contacts, and ribs run in both the crossed and perpendicular positions with respect to each other. Spacing, percent of the membrane area covered, and peripheral contact length were also varied. At the catalyst loadings in the range of interest, percent of the area covered was found a significant variable. Values below 3 percent and over 10 percent resulted in lower cell performance. This was explained by the high catalyst-surface resistance present at the lower values while at high-percent coverages too much of the catalyst surface was being masked from the reactive gases. Experiments indicated that there was little difference between the various shapes of the pickups compared at constant percent contact area. Crossed ribs seemed to give an output voltage about 3 percent lower than parallel ribs.

To effect a more significant electrochemical investigation of the cell performance, development of a miniature hydrogen reference-electrode has been undertaken. The reference electrode was mounted carefully in the 0.8 mm thick membrane so as not to be in direct electron-conducting contact with the two catalyst surfaces. While this development is not complete to the point of a satisfactory and complete check of the reference electrodes properties, the tentative results are given in Figure 9. With the standard catalysts used, practically all of the electrode (catalyst-layer) polarization was found at the oxygen catalyst-layer. A Tafel plot of the over-potential versus current-density *based on superficial electrode (catalyst) area* gave a slope of 0.072 in the range of variables investigated. Mercury penetrometer (porosimeter) measurements of the catalyst surface imbedded in the hydrated resin indicate an order of magnitude for the total surface areas of about 1000 cm^2 per cm^2 of superficial area. These values are roughly equivalent to 10 m^2 per gram of catalyst.

Life

During the past year a life testing program of the small 11.4 cm^2 cells* has been undertaken. Some cells have been operated continuously and intermittently for over a year on hydrogen and oxygen. It was found that total ampere-hours of operation was one of the main independent variables for predicting life of a given cell-construction. With these early types of membrane construction,

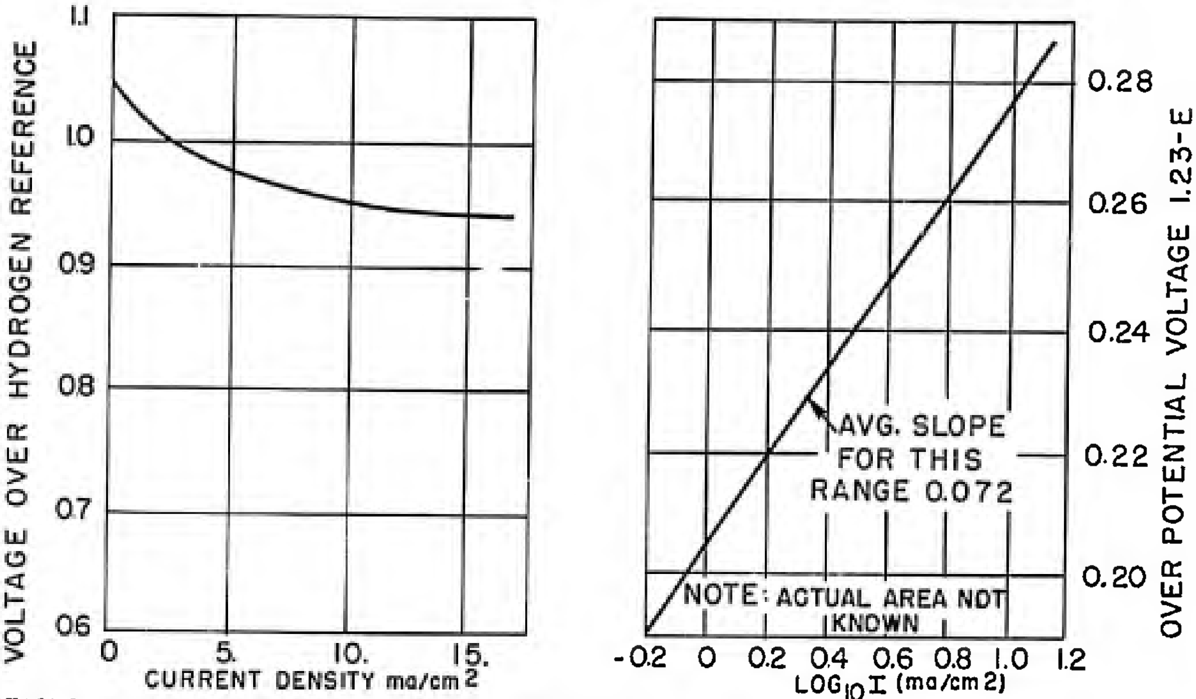

CONDITIONS: USING 1 ATM. H_2 & O_2, ROOM TEMPERATURE AMBIENT, 100 cm^2 SUPERFICIAL OXY. ELECTRODE AREA

Figure 9. Approximate oxygen electrode polarization.

life in excess of 30 ampere-hours per cm^2 of membrane surface (approx. 30,000 ampere-hours per square foot) were usually obtained with room-temperature ambients. With newer types of construction improved life is expected.

Construction

Certain stainless-steels, rubbers and common plastics have been found compatible with the cationic corrosive membrane. Conductive plastics and paints have been successful on limited tests. Titanium alloys are also likely candidates. Using these alloys for electrical pickups and cell construction involves a system optimization, between weight, cost, and ohmic loss. In the 200-watt unit, 4 mil-thick stainless steel is used for light-weight electrical pickups with the ohmic loss amounting to less than 5 percent of output.

Using the forementioned metal alloys in a "bipolar" designed cell stack along with optimized standard-catalyst loadings, a 50-to-one cost reduction in materials was obtained per unit area over the 11.4 cm^2 small cells discussed last year without any noticeable loss in cell performance. Preliminary experiments indicate a further materials cost-reduction of approximately five times is in the offing when experiments are completed using new catalyst systems. Since the General Electric Company has started to manufacture these membranes on a laboratory pilot-plant scale, changes in manufacturing methods have already cut the production time in half. In the future, continuous processing will reduce costs further.

Hydrogen Generation

To furnish pure moist hydrogen gas as fuel for the 200-watt fuel-cell, a totally-contained borohydride-acid system shown in Figure 10, was developed during the Fall of 1959. Borohydride was selected because of its known high specific hydrogen generation capability, especially in catalyzed acid solutions. Since there was also a −65F starting requirement, it was decided to meter 35 weight-percent sulfuric acid solution into small sodium-borohydride pellets to maintain a preset pressure at a low-pressure hydrogen-regulator input. Sulfuric acid was selected as a freezing point depressant because: (1) it had a low vapor pressure and would not contaminate the generated hydrogen; (2) only a 28 weight-percent increase over pure water was required; and (3) it added reactivity to the mixture at low temperatures. Experiments with the borohydride-acid system indicated that formation of certain hydrated sulfate and borate salts, stable 100°C, were blocking the reaction of the borohydride pellets. The inclusion of cobalt (II) chloride salts in the borohydride pellets greatly reduced the blockage with the cobalt entering into the boro-

---

*Described in Dr. Niedrach's 1959 paper.

hydride reaction and finally ending up as pink hydrated cobalt (II) sulfate. With a properly designed acid distributor moist hydrogen gases containing 50 cu ft (S.T.P.) of dry hydrogen were obtained from slightly less than 1.5 lb of sodium-borohydride pellets and slightly more than three pounds of 35 weight-percent sulfuric acid solution. The acid solution may be buffered with ferric ion to reduce corrosion with certain stainless-steels in long-term storage. At room-temperatures, the pellets generate hydrogen efficiently when mixed with water instead of sulfuric acid solution. No chloride ion and very little acid was found in a water bubbler through which the generated hydrogen gases passed.

Figure 10. Hydrogen generator canister reload for 14-hour operation contains 4.5 pounds of chemicals. It operates at low pressure (10-100 psig) to furnish 50 cu ft (STP) of hydrogen gas and will start generating at −65F.

Conclusion

In summary, this year's work has evaluated and indicated solutions to the significant problems connected with putting the G-E ion-exchange fuel-cell into a practical device for portable-power supplies. In particular, the achievement of practical current densities at reasonable voltages for cells of greatly enlarged area has been proven. Among the cell's advantages are silent operation and light weight.

Acknowledgement

The work outlined in this paper was accomplished principally by the General Electric Research Laboratory where this cell originated and the Aircraft Accessory Turbine Department where its further development has been taking place. Among the principal investigators at the Research Laboratory are W. T. Grubb, L. W. Niedrach, E. J. Cairns, D. L. Douglas and D. Sargent. At the Aircraft Accessory Turbine Department the following people were among those connected with work reported: A. P. Fickett, P. V. Popat, S. Bekelnitzky, W. A. Titterington, and R. H. Blackmer.

Application Information

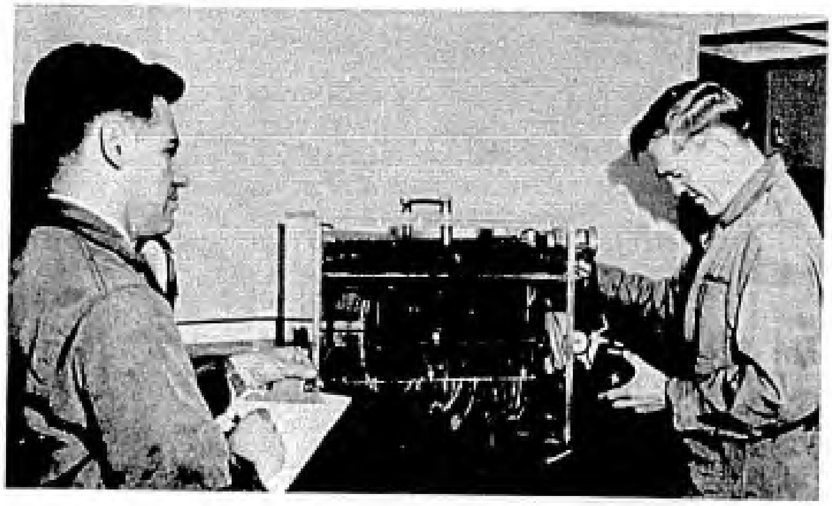

TESTING of twenty-five 90-sq in fuel cells in series at G-E's Aircraft Accessory Turbine Department

The portable power pack described in Dr. Oster's paper was developed for the U. S. Marine Corps and U. S. Army Signal Corps to power communication and radar equipment.

Individual fuel cells produce approximately one volt. Since their current depends on the area of the membrane, cells are presently being produced in sizes from four inches square to one foot square. Actually, there appears to be no theoretical limit on membrane area. But, practical considerations such as system reliability, thermal co-efficients, fabrication machinery and door widths will dictate the upper limits.

Being only 1/8-1/4 inch thick, cells can be stacked in modules — series or parallel — to form useful blocks of power that are subject to the same rules as conventional batteries. System reliability obviously favors several modules in parallel rather than one large bank in series. So, for installations less than 1 kw, it appears that the largest membrane size will be in the order of two-feet square, or less.

Although General Electric is not yet offering fuel cells for off-the-shelf sale, inquiries concerning the application of present technology or development of specialized power packages are invited. If you are considering the use of this type of equipment, please contact your nearest Aircraft Accessory Turbine Department Representative.

AIRCRAFT ACCESSORY TURBINE DEPARTMENT SALES OFFICES

CALIFORNIA, Los Angeles	3325 Wilshire Boulevard	DUnkirk 1-3641
CALIFORNIA, San Diego	3636 Fifth Avenue	CYpress 7-2911
DISTRICT OF COLUMBIA, Washington 5	777 - 14th Street, N.W.	EXecutive 3-3600
KANSAS, Wichita 2	200 E. First Street	AMherst 7-4263
MASSACHUSETTS, Lynn 3	950 Western Avenue, Bldg. 1-74A	LYnn 8-6000, Ext. 5433
MISSOURI, St. Louis 21	4790 St. Andrew Street, Bridgeton	PErshing 1-4343
NEW YORK, Garden City, L. I.	600 Old Country Road, Rm. 232	PIoneer 7-6300
OHIO, Cincinnati 15	Lockland Highway, Bldg. 100	POplar 1-4100, Ext. 1636
OHIO, Dayton 2	118 West First Street	BAldwin 3-7151
OKLAHOMA, Midwest City	213 Post Office Bldg.	PErshing 2-4567
WASHINGTON, Seattle 8	220 Dawson Street	PArkway 5-6800

CANADA

Canadian General Electric Co., Ltd. 830 Lansdowne Avenue, Toronto: LEnox 4-6511

EUROPE

General Electric Co. 1 rue du Temple, Geneva, Switzerland: 326276